On the role and morphology of the magnetic field during flares in Blazars

Collaborators:

K P Singh (TIFR), Markus Bottcher (NWU), Haocheg Zhang (LANL)
David A. H. Buckley (SAAO), Pankaj Kushwaha (TIFR),
C. Stalin (IIA), K. S. Baliyan (PRL,MIRO)

Sunil Chandra
TIFR-Mumbai, India

Blazars

A Relativistic Jet closely aligned to LOS

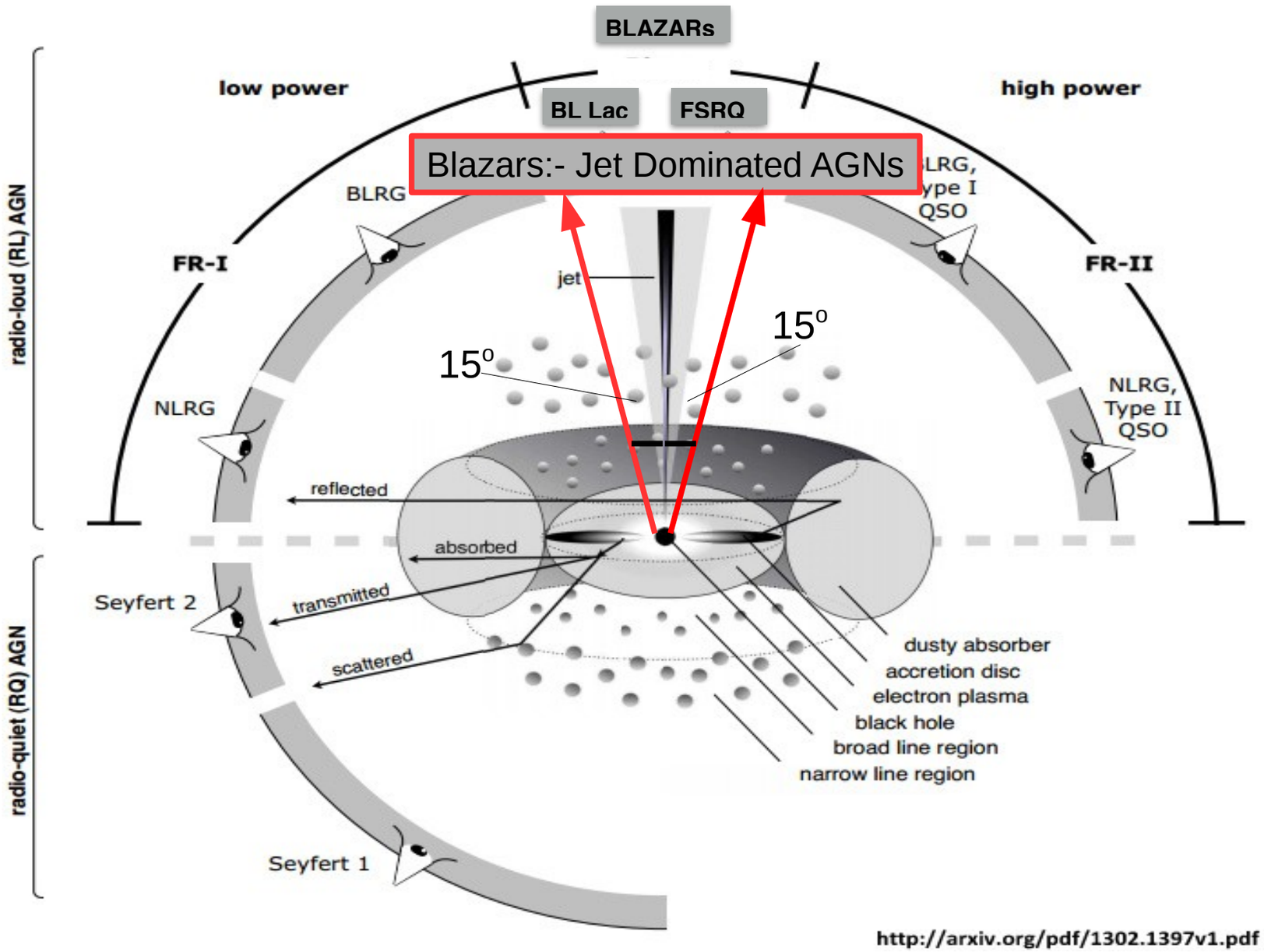

http://arxiv.org/pdf/1302.1397v1.pdf

Blazars

A Relativistic Jet closely aligned to LOS

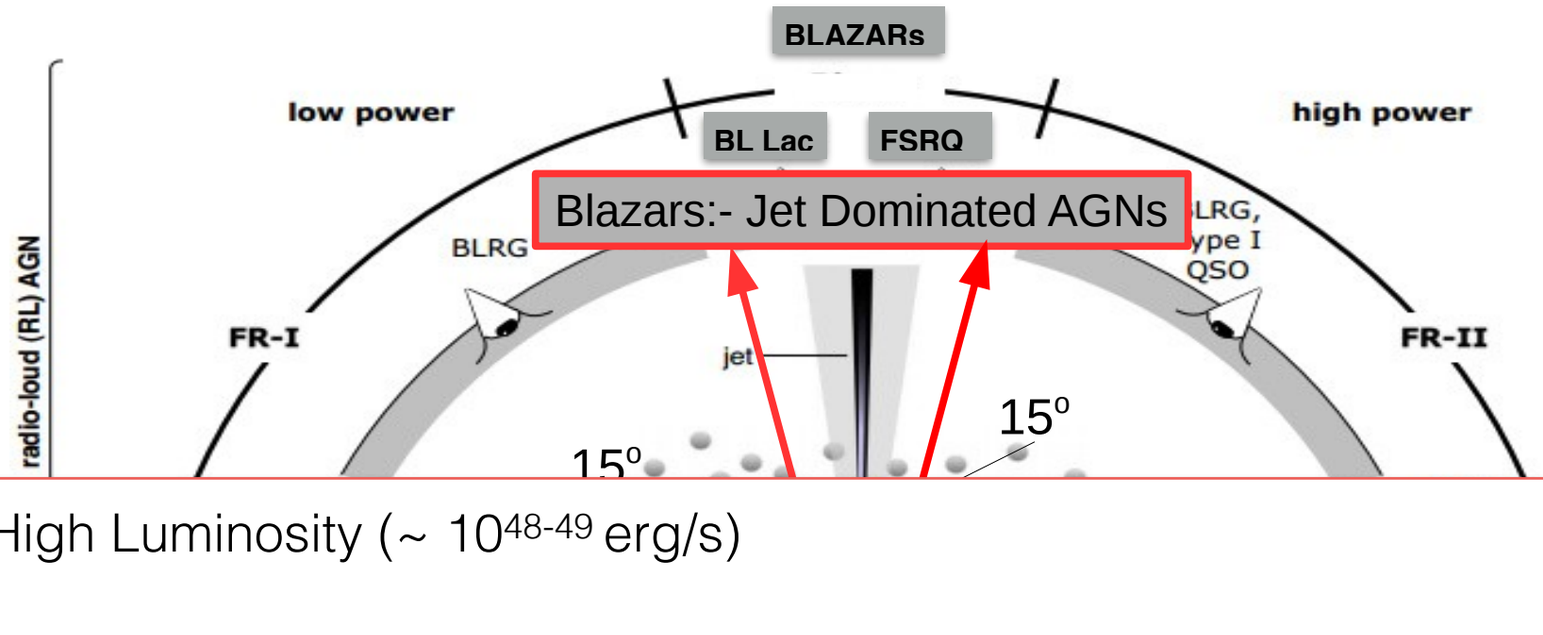

- High Luminosity (~ $10^{48\text{-}49}$ erg/s)
- Broad-Band Spectral Energy Distribution (SED)
- Very weak or featureless optical/UV spectra
- violent variability through the entire electromagnetic spectrum at different timescales (from years down to TeV flares of ~ 5 min duration)
- strong and variable linear polarization from radio to UV wavelengths (up to 40%, Jostad et al. 2006 & 38 % for OJ 287 from MIRO)

Low-frequency peaked / Intermediate BL Lacs (LBLs/ IBLs):

Peak frequencies at IR/ Optical and GeV gamma-rays,

10^{14} Hz < ν_{sy} ≤ 10^{15} Hz

Intermediate overall luminosity

Sometimes γ-ray dominated

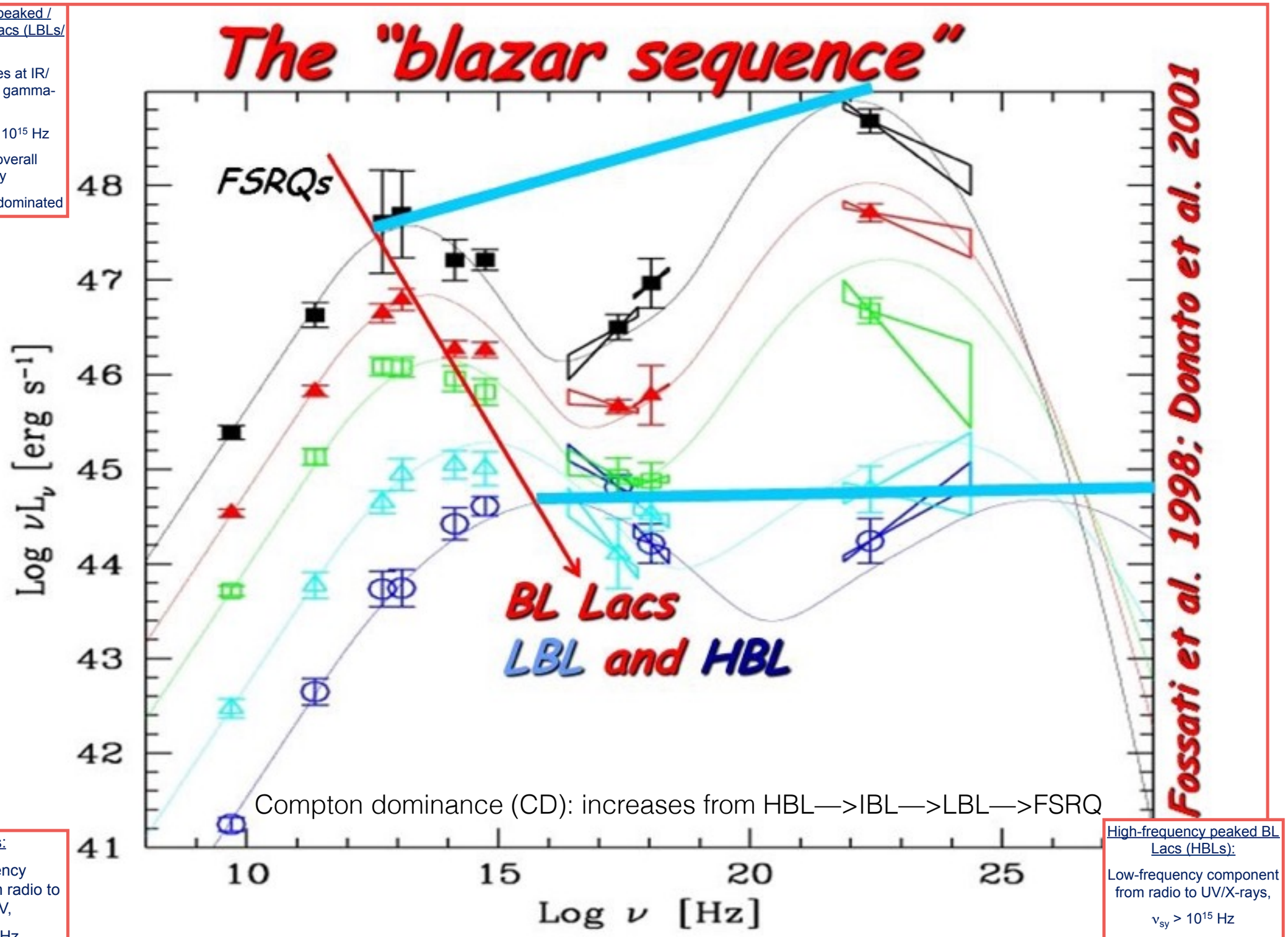

Compton dominance (CD): increases from HBL—>IBL—>LBL—>FSRQ

Quasars:

Low-frequency component from radio to optical/UV,

ν_{sy} ≤ 10^{14} Hz

High-frequency component from X-rays to γ-rays, often dominating total power

High-frequency peaked BL Lacs (HBLs):

Low-frequency component from radio to UV/X-rays,

ν_{sy} > 10^{15} Hz

often dominating the total power

High-frequency component from hard X-rays to high-energy gamma-rays

Content

- Introduction of the conventional SED modelling
- Importance of the magnetic fields
- How can we understand the morphology of the magnetic field, during flares ?
- The historical flare of S5 0716+714 in 2015
- Hope for a better understanding of blazars and underlying processes using AstroSat + Ground based observatory consortium (SALT, MIRO, HCT, ARIES +…)

Blazars: SED - Modeling

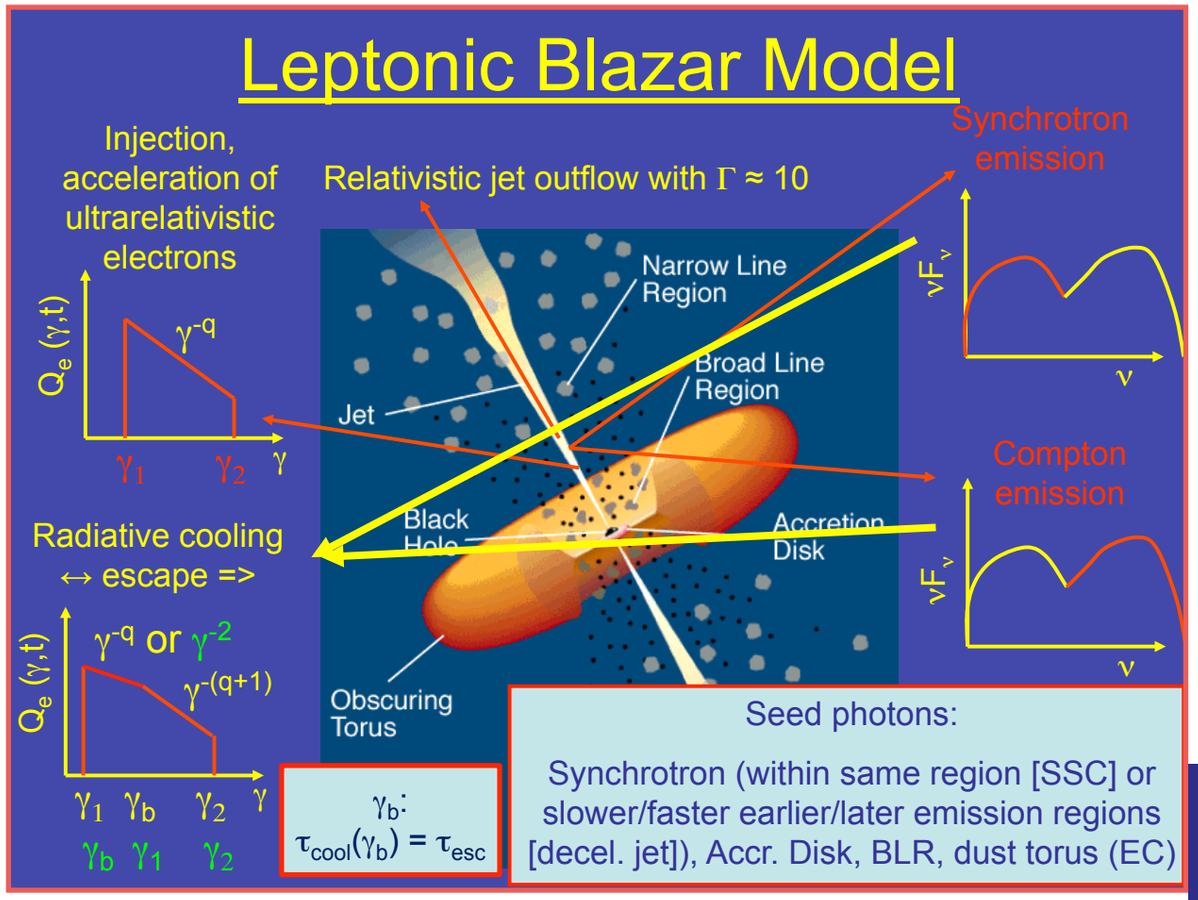

Leptonic Models

-20

Hadronic Models

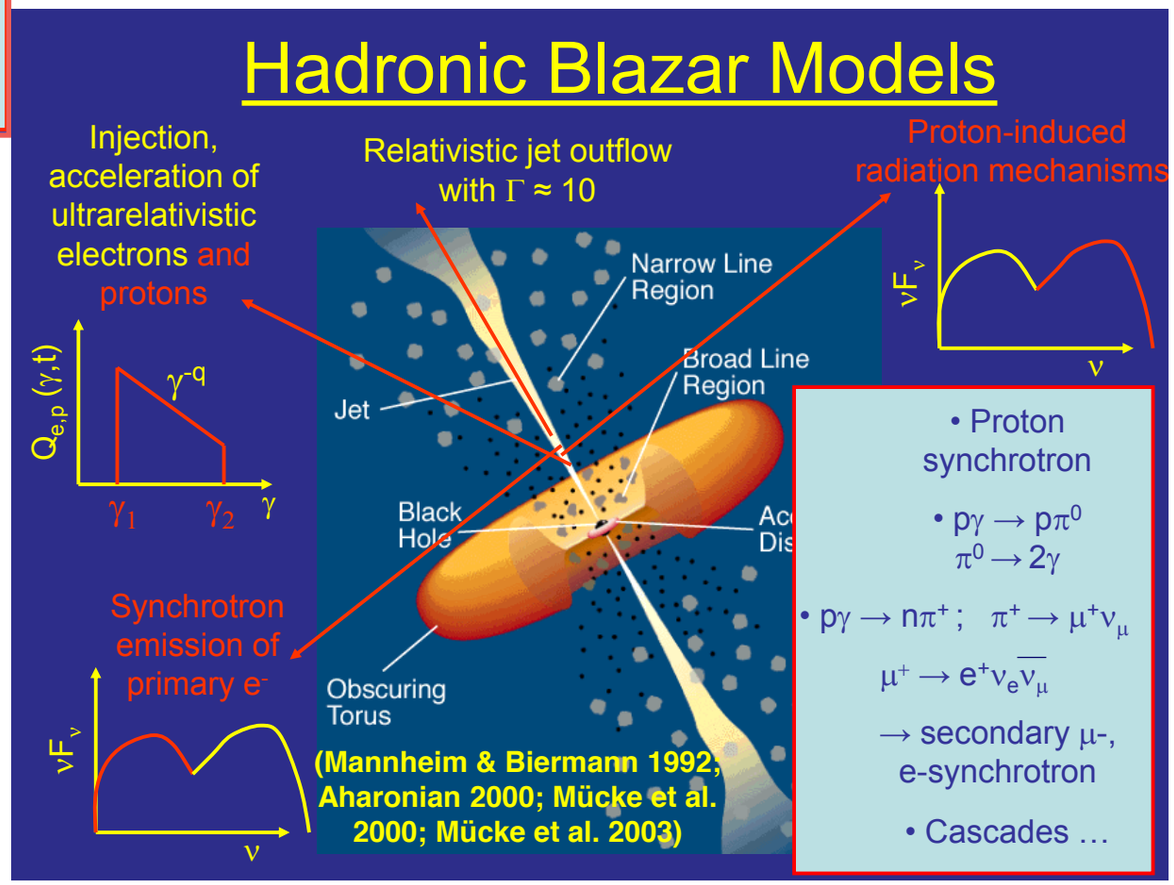

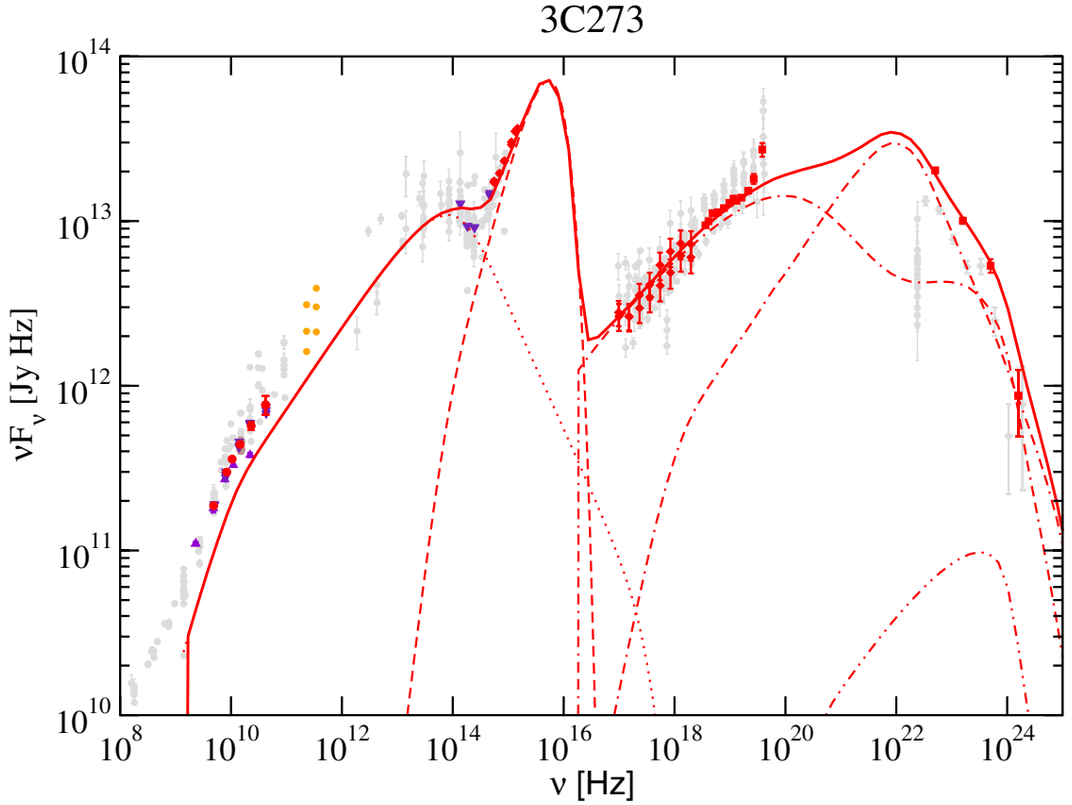

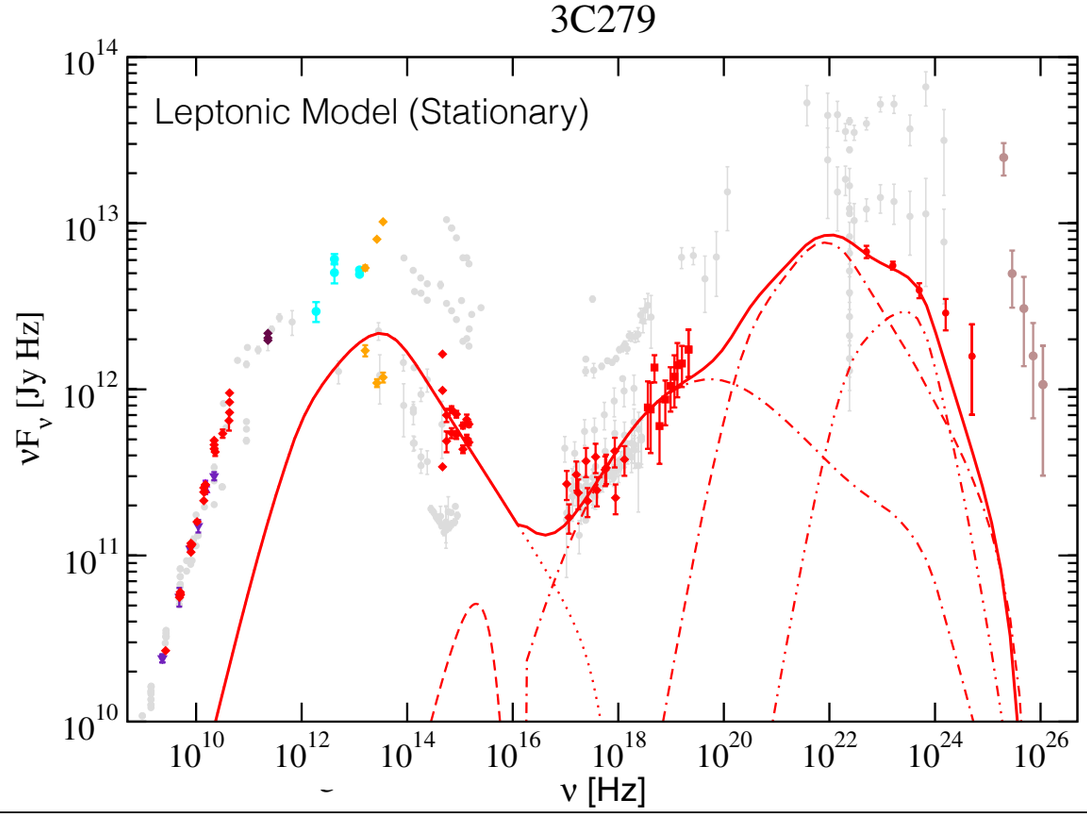

Object	$\gamma_{e,1}$	$\gamma_{e,2}$	q_e	B [G]	D	$f_{\rm BLR}$[a]	L_e[b]	L_p[b]	L_B[b]	ϵ_{Be}	$t_{\rm var,min}$[c]
3C 273	1×10^3	5×10^4	3.5	2.0	13	5.4×10^{-5}	6.0	130	0.63	0.11	4.1
3C 279	1×10^3	1×10^5	3.0	0.7	17	1.7×10^{-2}	5.8	29	5.4	0.94	29

Object	$\gamma_{e,1}$	$\gamma_{e,2}$	q_e	B[a]	D	$\gamma_{\rm p,max}$	q_p	L_e[b]	L_p[c]	ϵ_{Be}[d]	ϵ_{Bp}[d]	ϵ_{ep}[d]	$t_{\rm var}$[e]
3C 273	350	1.5×10^4	3.4	15	15	4.3×10^8	2.4	0.13	25	3300	1.7×10^{-3}	5.2×10^{-7}	11
3C 279	100	2.0×10^4	3.0	100	15	6.4×10^8	2.2	0.19	3.5	1410	7.9×10^{-3}	5.6×10^{-6}	1.7

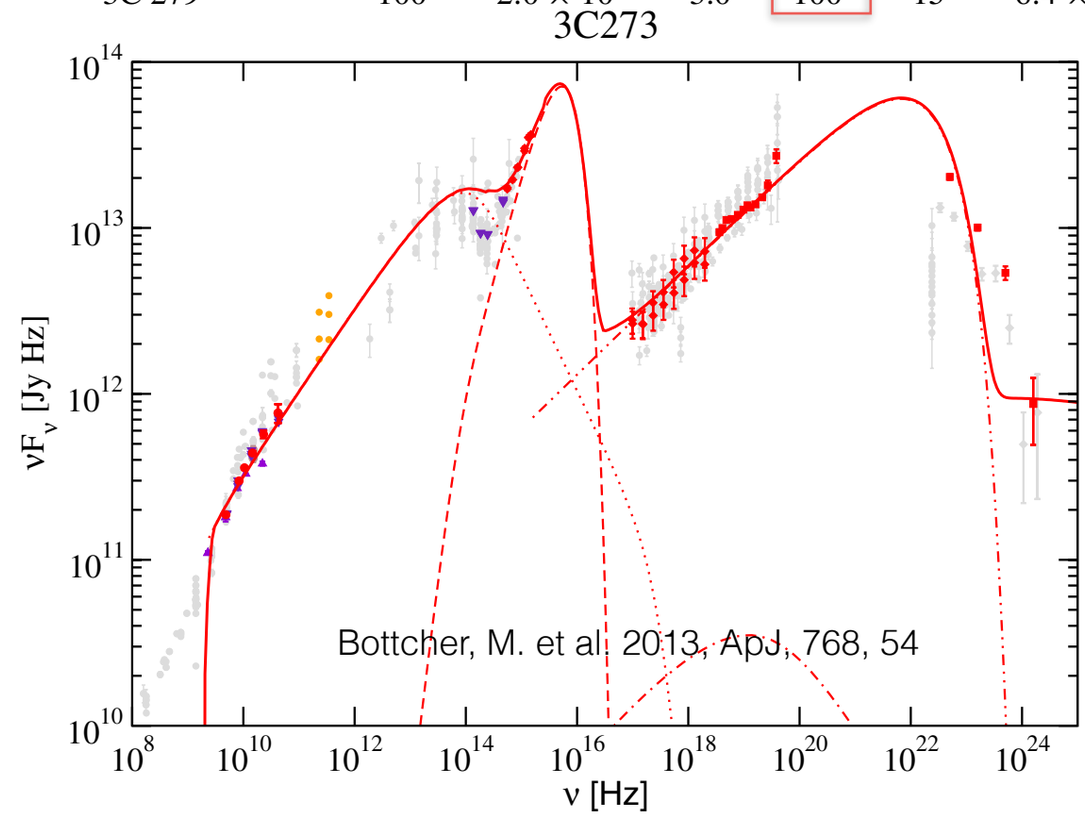

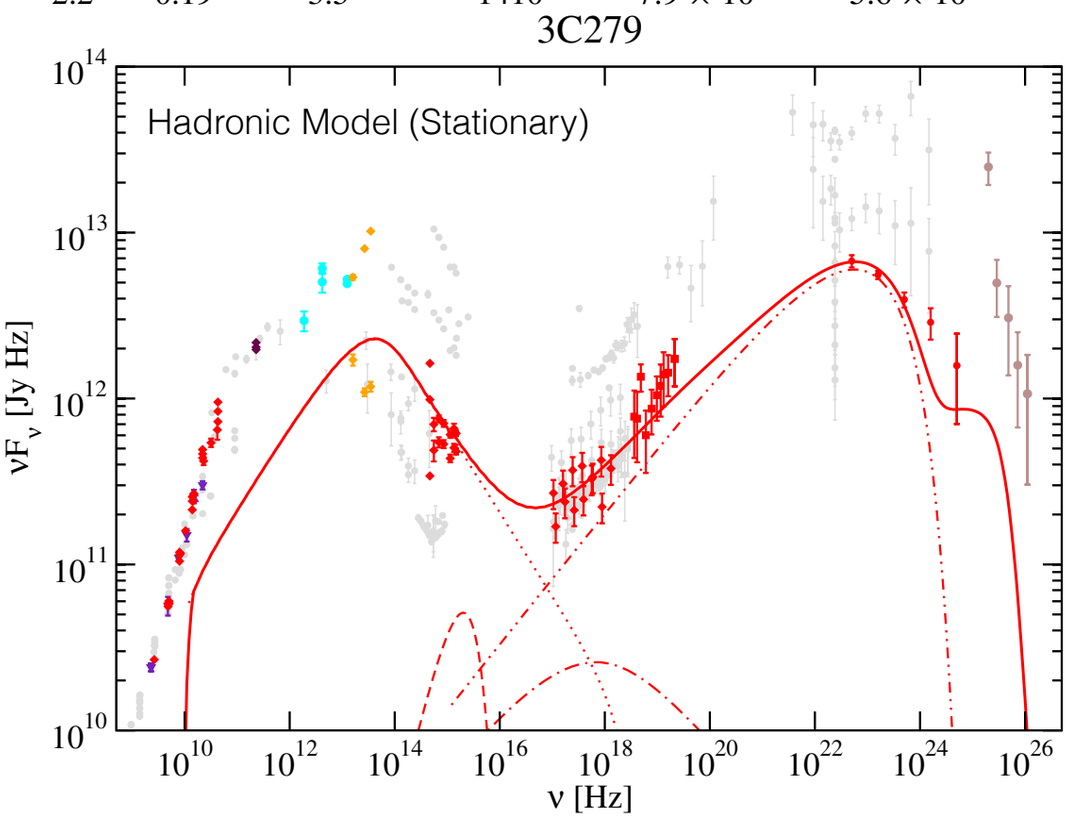

Time-Independent Leptonic Model & SEDs; PKS 1510-089 (z~0.361)

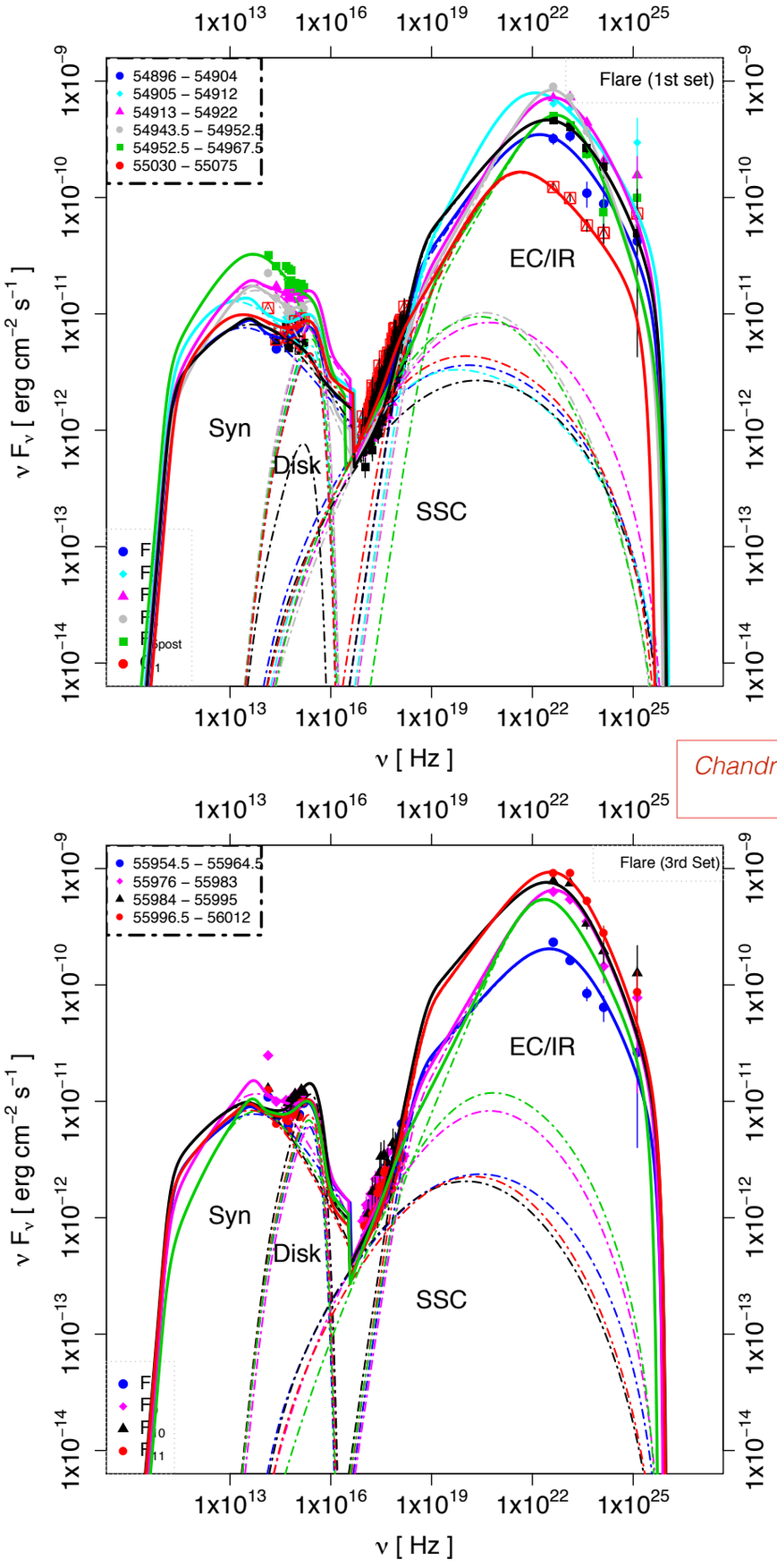

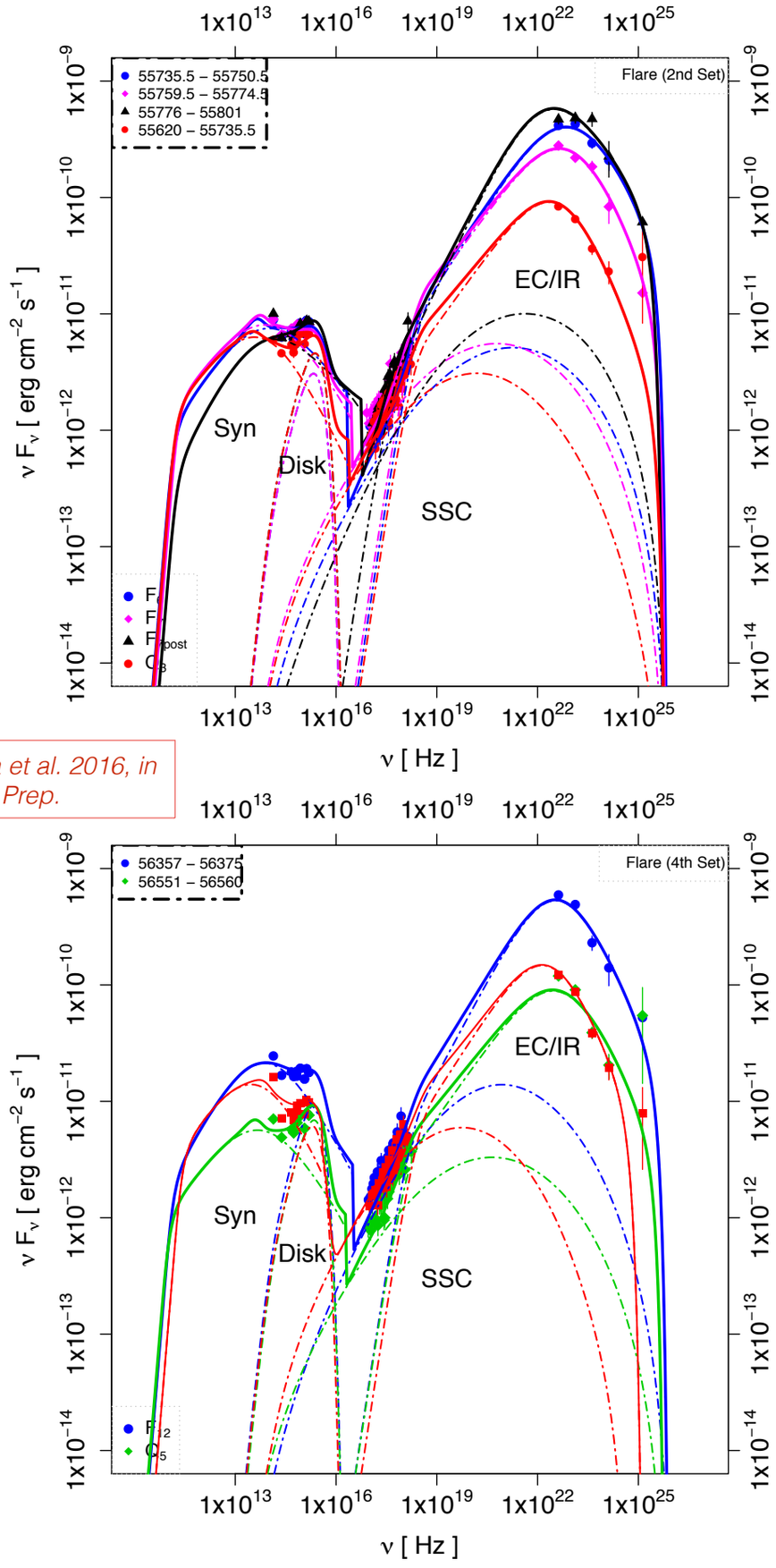

Chandra et al. 2016, in Prep.

Assumptions:

Emission Region : Circular

Within or beyond BLR

Magnetic field is large scale no special consideration about morphology

Protons in the emission region are cold enough and do not contribute to the radiative emission significantly

Time averaged behaviour for the duration of the SED …no information about particle evolution

Time-Dependent Leptonic / Hadronic Models

Single v/s Multi zone

Simultaneous modelling of SED light curves and polarisation

Optical Polarisation; CGRaBS J0211+1051

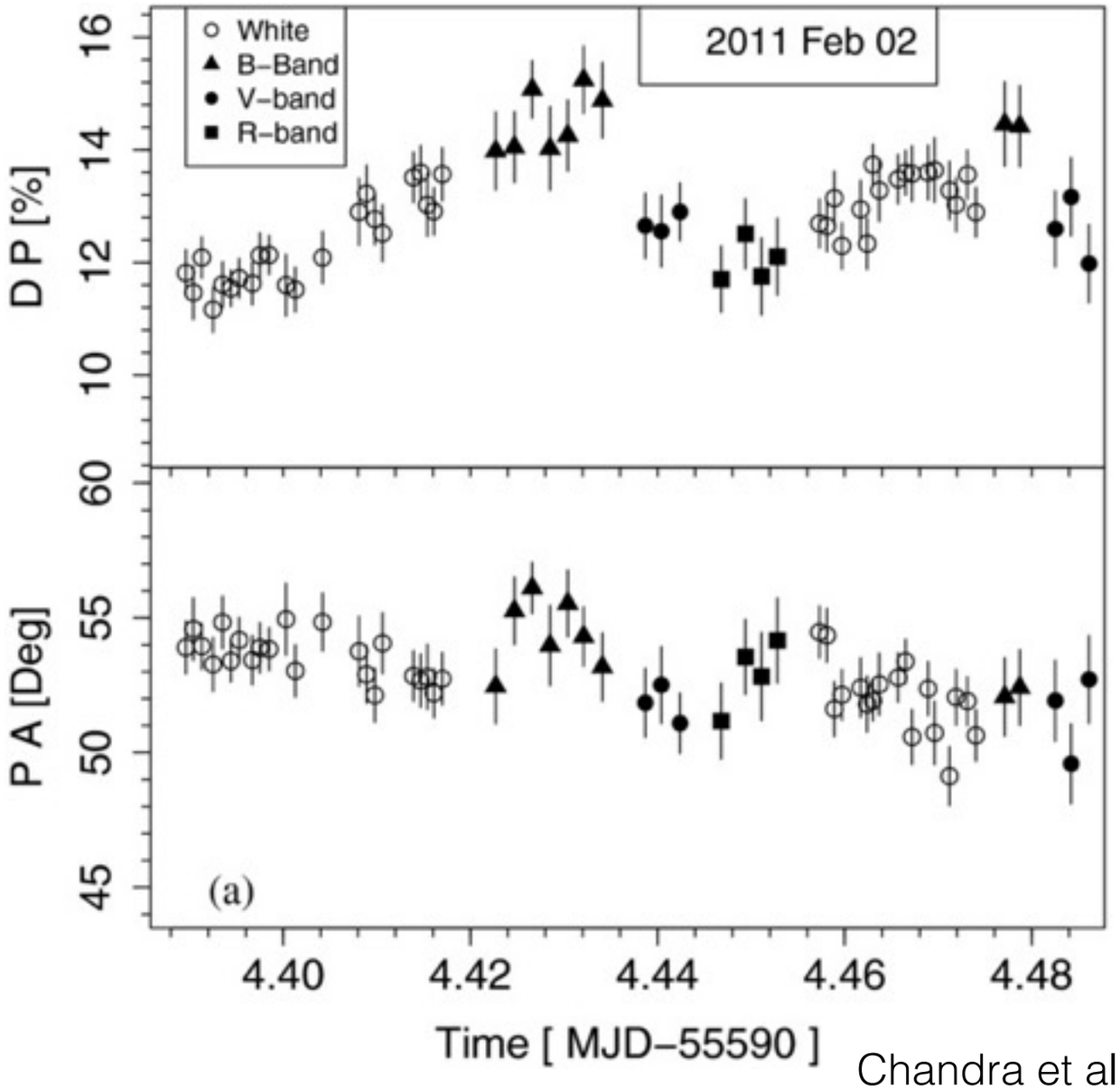

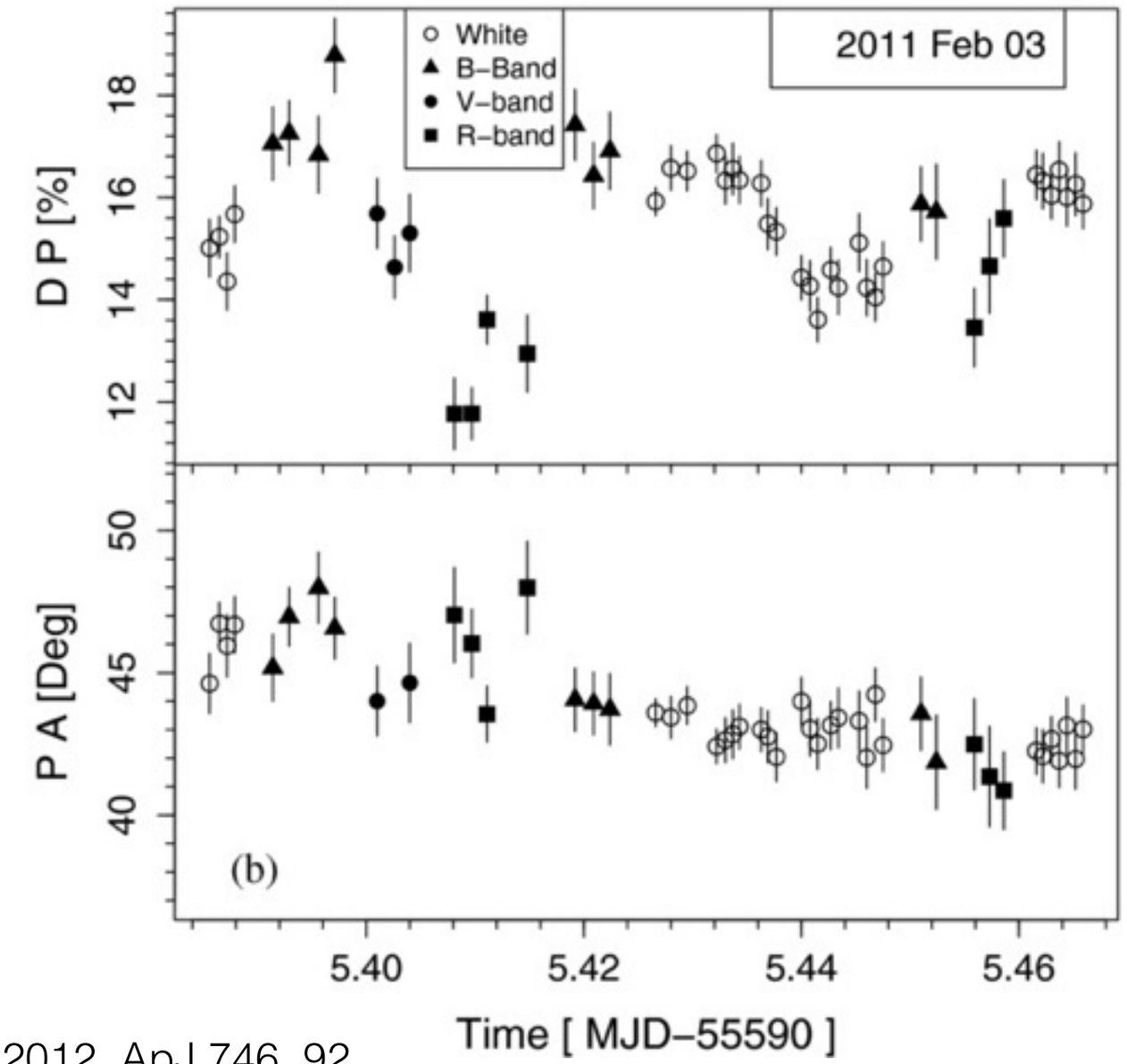

Chandra et al. 2012, ApJ 746, 92

3C 279 (z~0.536)

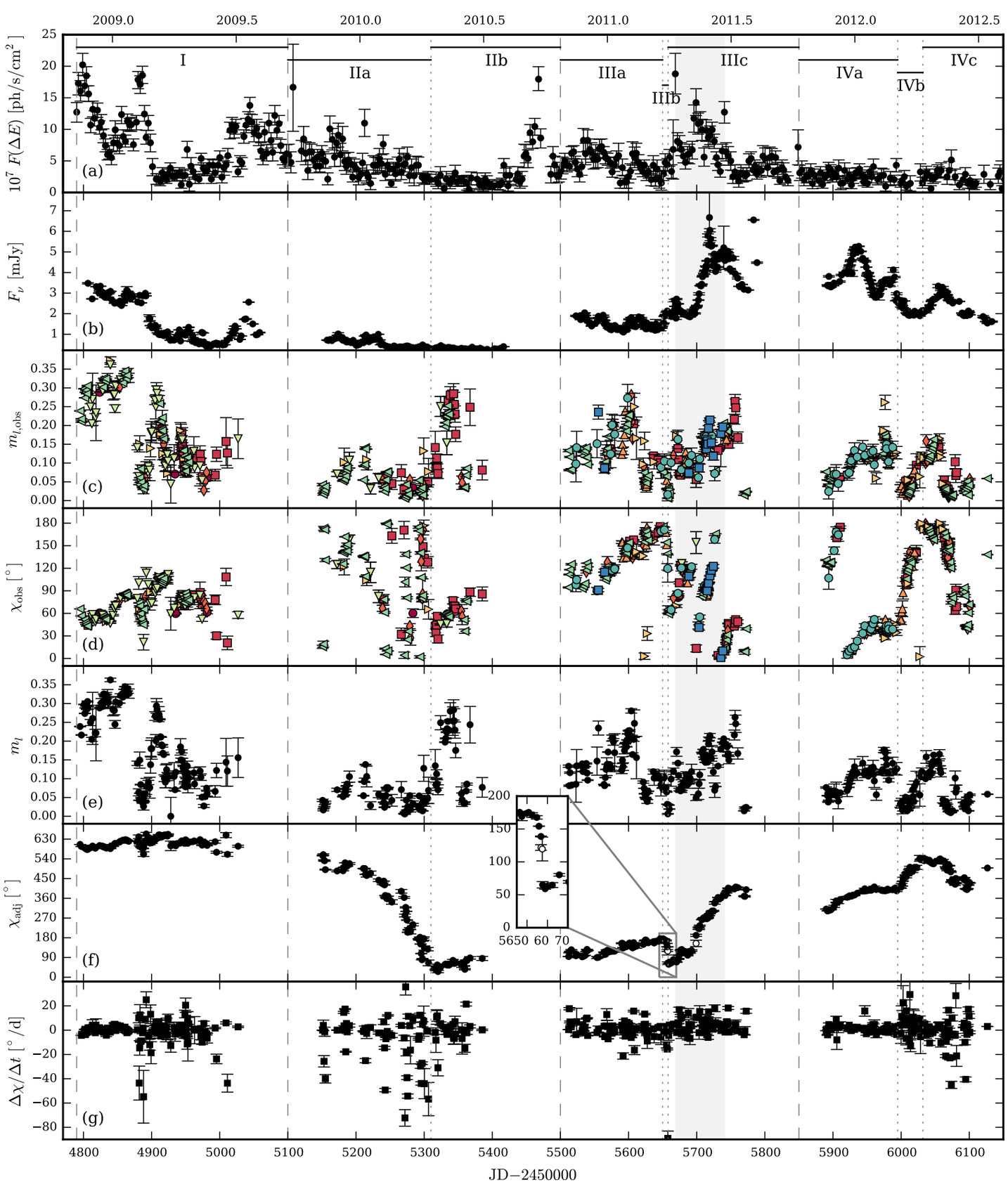

Fig. 1. Optical photometry and polarimetry and γ-ray light curve of 3C 279. Fermi-LAT γ-ray light curve at > 100 MeV binned into 3 day intervals (panel a) as published in Hayashida et al. (2015). Combined *R*-band light curve (panel b). Measured, optical polarization fraction (panel c) and EVPA (panel d); red circles: Calar Alto (R), red squares: CrAO-70cm (R), red diamonds: Perkins (R), orange up-sided triangles: SPM (R), orange right-sided triangles: St. Petersburg (R), green down-sided triangles: KANATA (V), green left-sided triangles: Steward Obs. (spec. and V), blue circles: Liverpool (V+R), blue squares: KVA (white light). Combined, de-biased, and averaged polarization fraction (panel e). Combined, averaged, and adjusted EVPA (panel f); open symbols are added from the non-averaged EVPA curve. Pointwise, local derivative of the adjusted EVPA (panel g). The grey area highlights the period of γ-ray flaring activity coinciding with a rotation of the optical polarization angle.

Kiehlmann et al 2016, arXiv: 1603.00249v1

A lot of polarisation angle rotation events during or near to a flare…

A lot of polarisation angle rotation events… sometimes even > 180°

Geometry dependent models

Radiative processes dependent Model

Geometry based models need more than one emission regions to pass through the bent of the jet in a fashion to give rise consistent rotations of ~ 360°

Looks a bit complex

Simultaneous modelling of SED light curves and polarisation, TEMZ and HMFM

TEMZ: Turbulent Extreme Multi-Zone Model

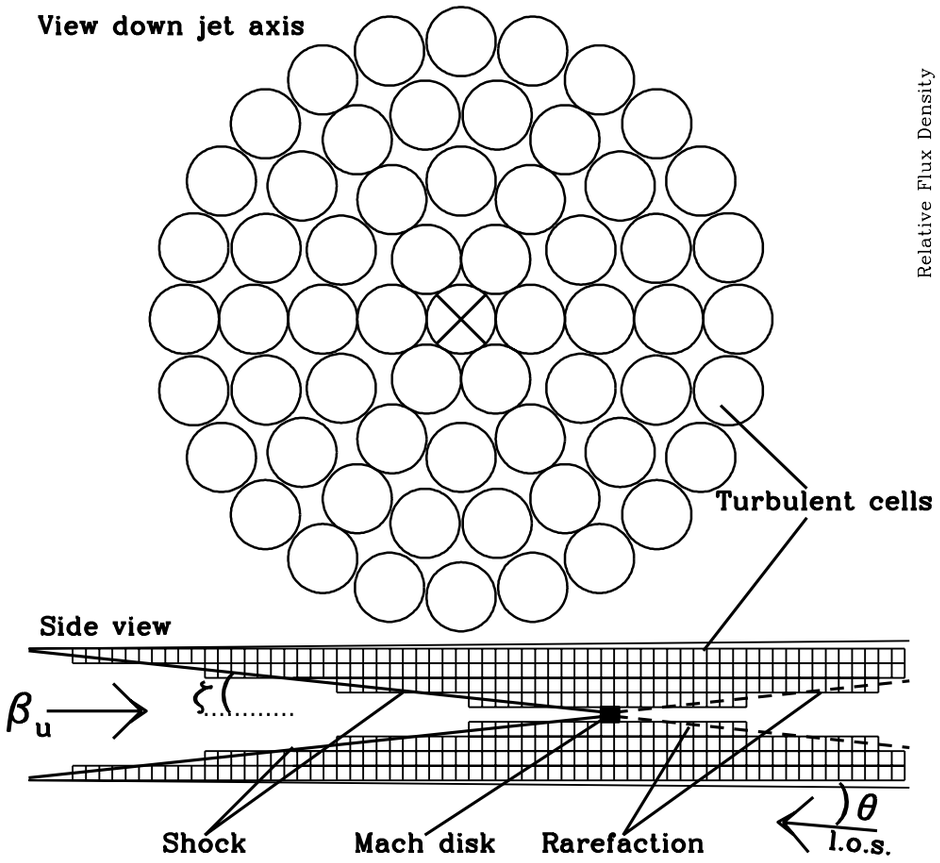

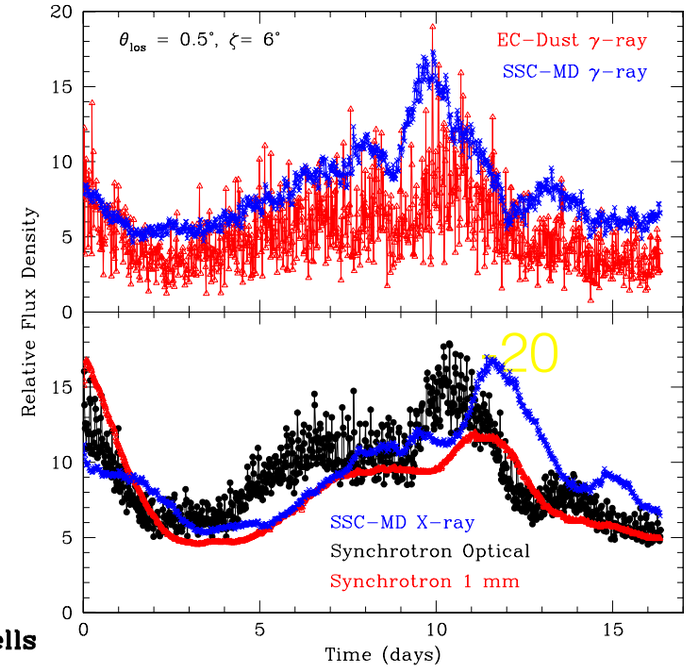

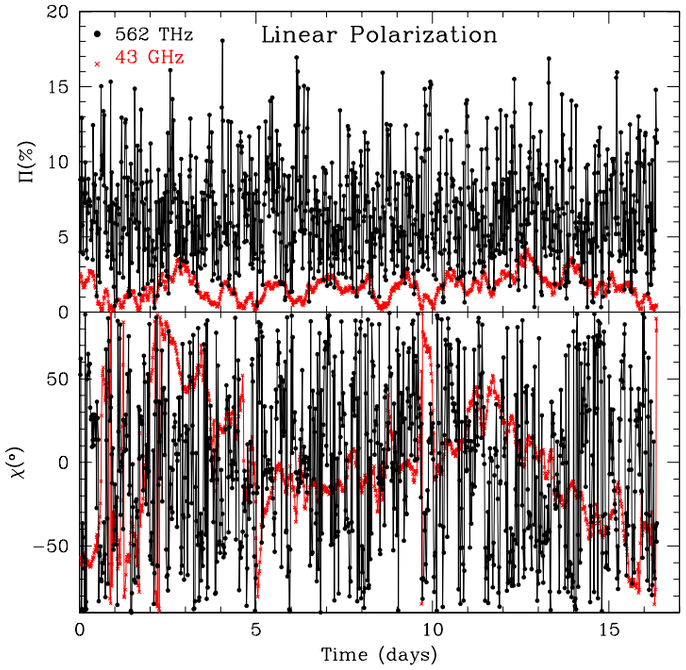

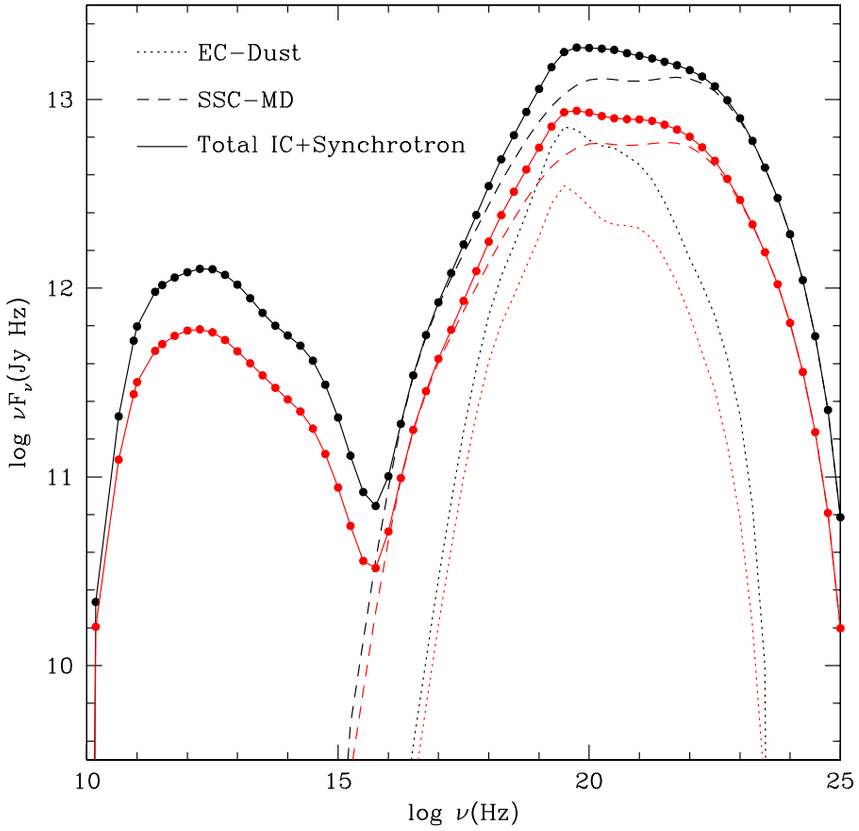

Fig. 1.— Sketch of the geometry employed to carry out calculations within the TEMZ code. The number of fixed computational cells across the jet cross-section (view down axis, in which × marks the Mach disk) can be as high as 1140, not including the Mach disk. A turbulent cell of plasma, moving at laminar velocity β_u upstream of the shock and at laminar velocity β_d after it passes the shock, crosses one computational cell during each time step. The emission occurs between the conical standing shock and the rarefaction. The entire region sketched lies $\gtrsim 1$ pc from the central engine.

parameters selected to be similar to PKS 1510−089: $n_{\rm rad} = 10$ (270 cells across the shock front), $z_{\rm MD} = 1.18$ pc, $Z = 0.361$, $\alpha = 0.7$, $b = 1.7$, $B = 0.04$ G, $f_B = 1.0$, $R_{\rm cell} = 0.001$ pc, $\gamma_{\rm min} = 1800$, $\gamma_{\rm max,high} = 37,500$, $\gamma_{\rm max,low} = 5000$, $\beta_u = 0.99969$, $\beta_t = 0.577$, $\zeta = 6°$, $\theta_{\rm los} = 0.^\circ5$, $\phi = 0.^\circ2$, $A_{\rm MD} = 1$, $T_{\rm dust} = 1200$ K, $L_{\rm dust} = 1 \times 10^{46}$ erg s^{-1}, $r_{\rm dust} = 3.0$ pc, and $R_{\rm dust} = 0.8$ pc. The SEDs correspond to times of 3.0 days (red) and 10.0 days (black). The temporal resolution is 0.0159 days (23 minutes) over 1027 time steps.

HMFM: Helical Magnetic Field Model

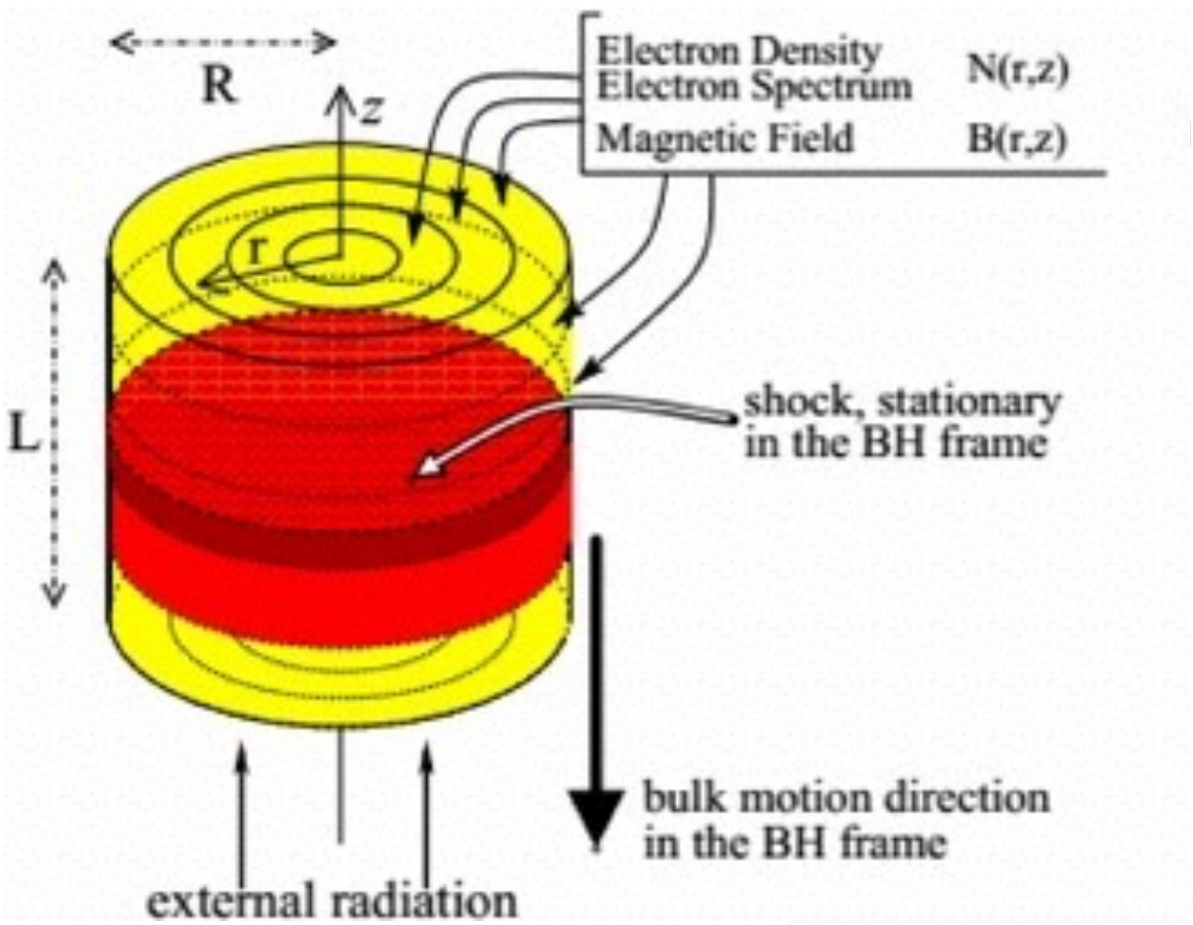

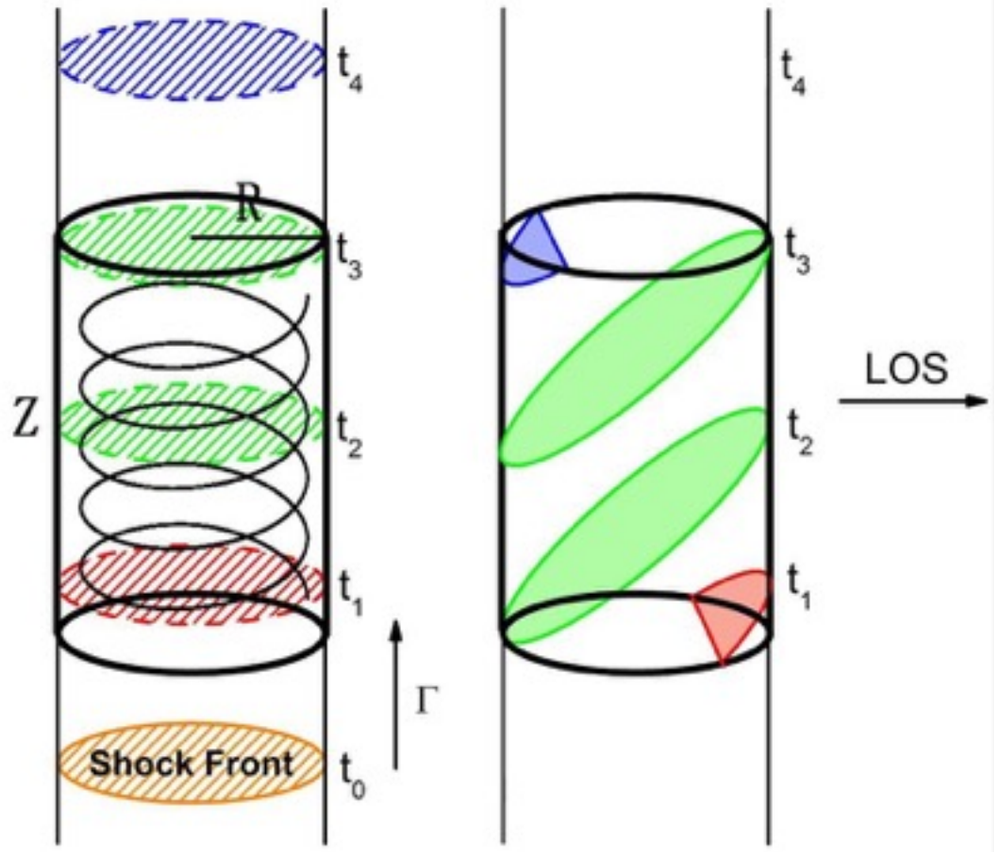

Haocheng et al. 2014, 2015

Large scale helical magnetic field

Cylindrical emission region

Simultaneous flux & polarization

3C 279, 2010 flare using HMFM

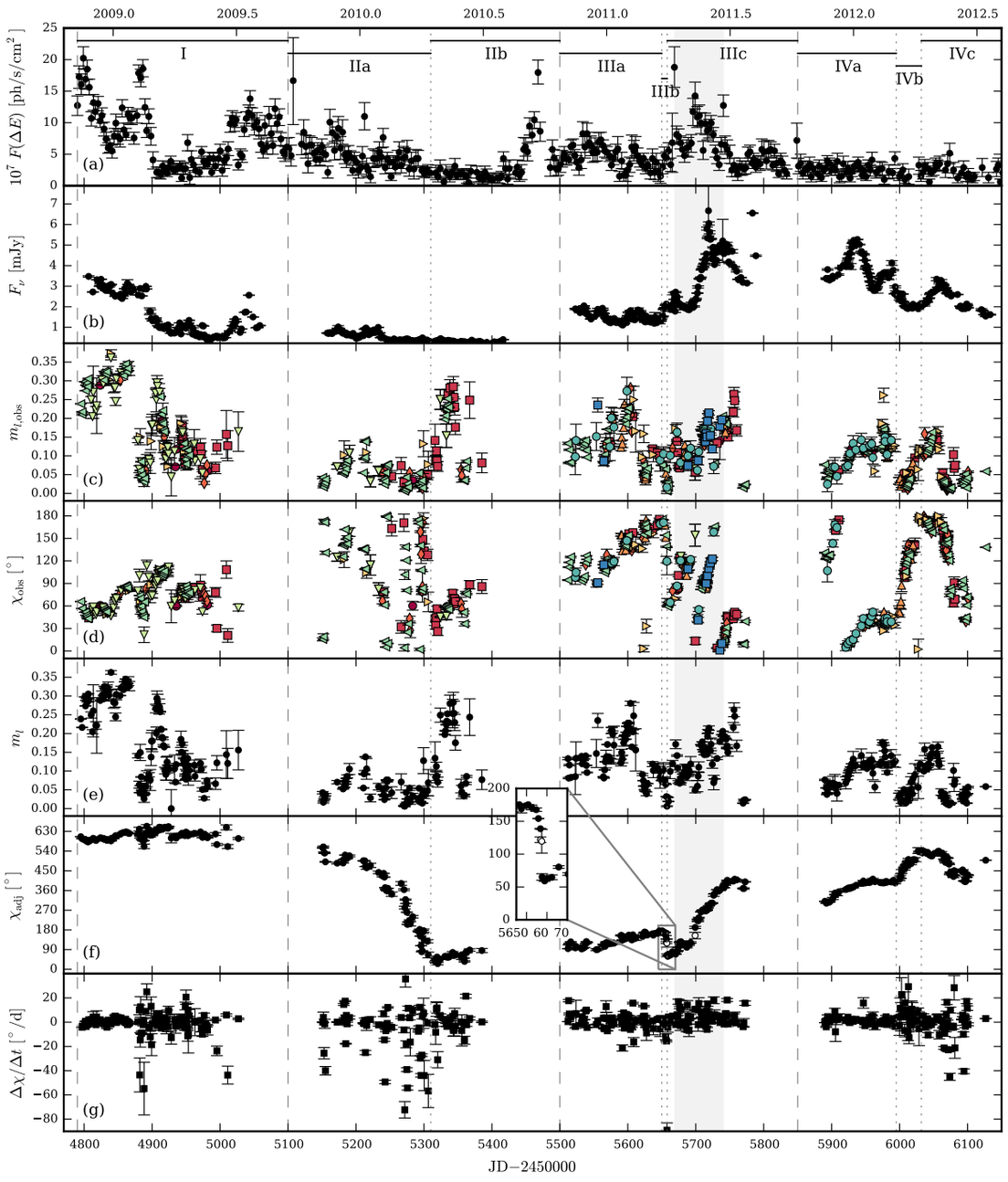

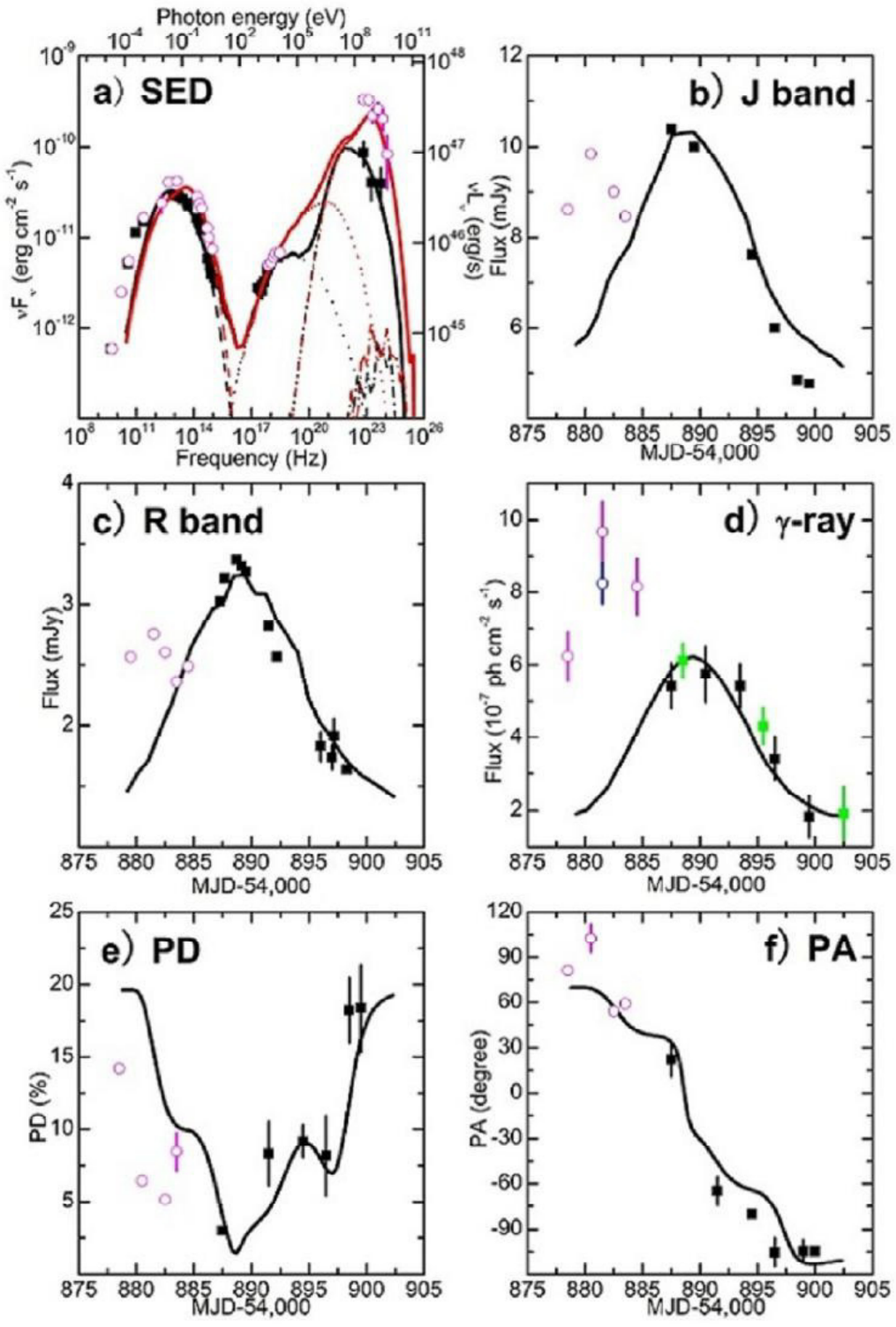

Fig. 1. Optical photometry and polarimetry and γ-ray light curve of 3C 279. Fermi-LAT γ-ray light curve at > 100 MeV binned into 3 day intervals (panel a) as published in Hayashida et al. (2015). Combined *R*-band light curve (panel b). Measured, optical polarization fraction (panel c) and EVPA (panel d); red circles: Calar Alto (R), red squares: CrAO-70cm (R), red diamonds: Perkins (R), orange up-sided triangles: SPM (R), orange right-sided triangles: St. Petersburg (R), green down-sided triangles: KANATA (V), green left-sided triangles: Steward Obs. (spec. and V), blue circles: Liverpool (V+R), blue squares: KVA (white light). Combined, de-biased, and averaged polarization fraction (panel e). Combined, averaged, and adjusted EVPA (panel f); open symbols are added from the non-averaged EVPA curve. Pointwise, local derivative of the adjusted EVPA (panel g). The grey area highlights the period of γ-ray flaring activity coinciding with a rotation of the optical polarization angle.

• 2015, January outburst in BL Lac object S5 0716+714

- S5 0716+714 (z~0.31; Nilsson et al. 2008, Mazin et al. 2009) [z<0.322 (95% confidence); Danforth et al. 2002]
- Most active blazar of extreme northern sky (RA 07:21:53.4 DEC +71:20:36) observed over complete spectrum
- Various Detections by EGRET (2E 0716.2+7126, 2EG J0720+7126, 3EG J0721+7120, EGR J0723+7134)
- Member of Fermi LAT Bright Source List (FERMILBS) F ~ 1.5 x 10^{-7} ph cm^{-2} s^{-1}
- Variable TeV detection by (Sp. Index=-3.45 +/- 0.54) MAGIC in 2007 November ($F_{>0.4TeV} \sim 0.8 \times 10^{-11}$ erg cm^{-2} s^{-1}) & 2008 April ($F_{>0.4T\,eV} \sim 7.5 \times 10^{-11}$ erg cm^{-2} s^{-1}) [Anderhub et al. 2009] with corresponding variability in optical bands (20 mJy to 45 mJy in V). A historical bright state in X-Rays during 2008 outburst [Giommi et al.2008].

Optical observations (R-Band)

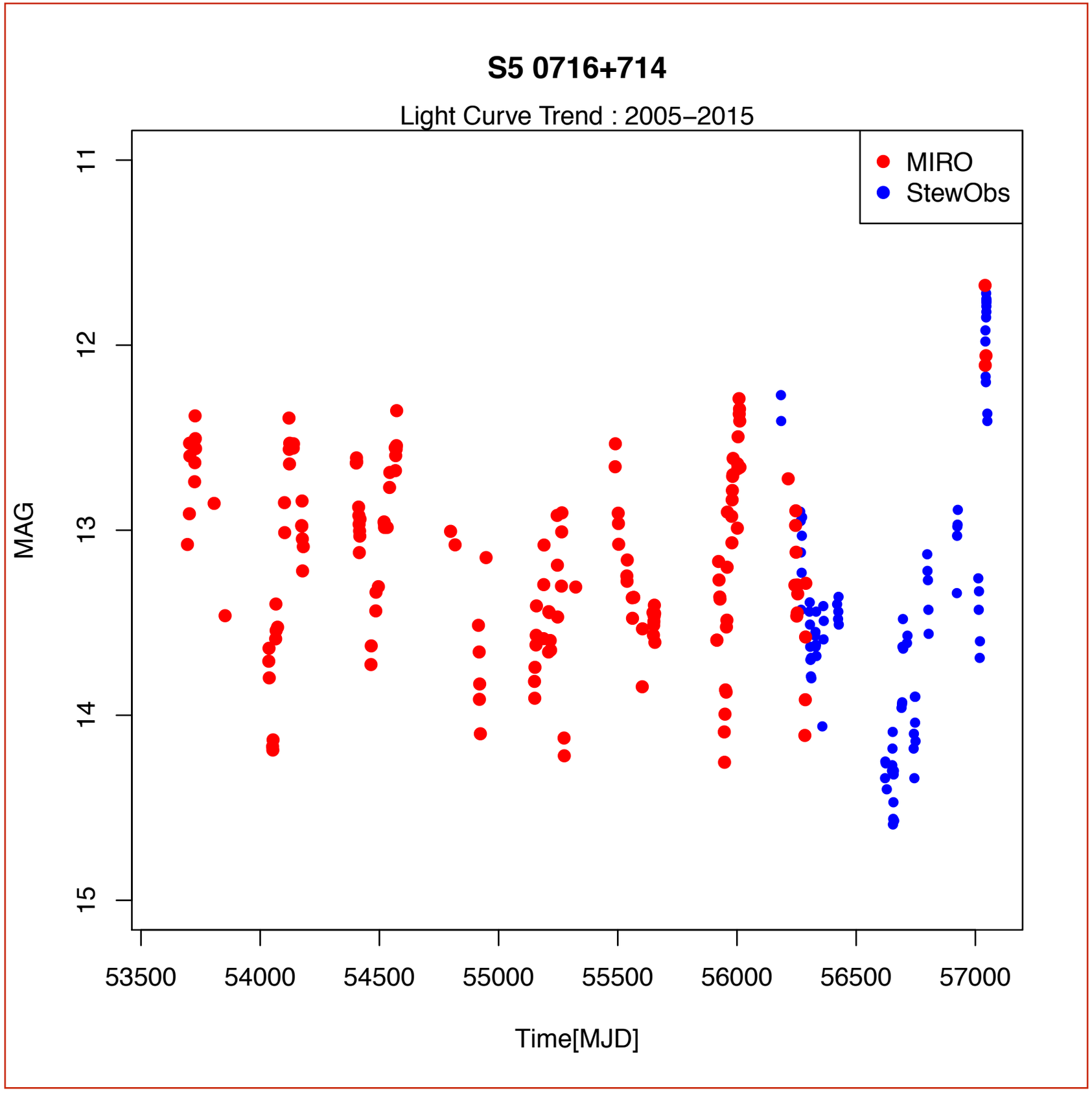

An ongoing NIR Flare of the Blazar HB89 0716+714

ATel #6902; *L. Carrasco, A. Porras, E. Recillas, J. Leon-Tavares, V. Chavushyan, A. Carraminana (INAOE, Mexico)*
on ***12 Jan 2015; 02:56 UT***

The blazar S5 0716+714 at the highest optical flux ever reported.

ATel #6957; *R. Bachev, A. Strigachev (IA-NAO, BAS, Bulgaria)*
on ***19 Jan 2015; 21:26 UT***

Unprecedented brightening of blazar S5 716+714 and a brighter CGRaBS J0510+1800

ATel #6962; *Sunil Chandra (TIFR, Mumbai), Pankaj Kushwah(TIFR, Mumbai), S. Ganesh(PRL, Ahmedabad), Navpreet Kaur(PRL, Ahmedabad), Kiran Baliyan(PRL, Ahmedabad, India)*

MAGIC detects Very High Energy gamma-rays from S5 0716+714

ATel #6999; *Razmik Mirzoyan on behalf of the MAGIC collaboration*
on ***27 Jan 2015; 20:02 UT***
Credential Certification: Razmik Mirzoyan (Razmik.Mirzoyan@mpp.mpg.de)

Multi-wavelength Lightcurves S5 0716+714 (z~0.31), 2015 January 23 - February 03

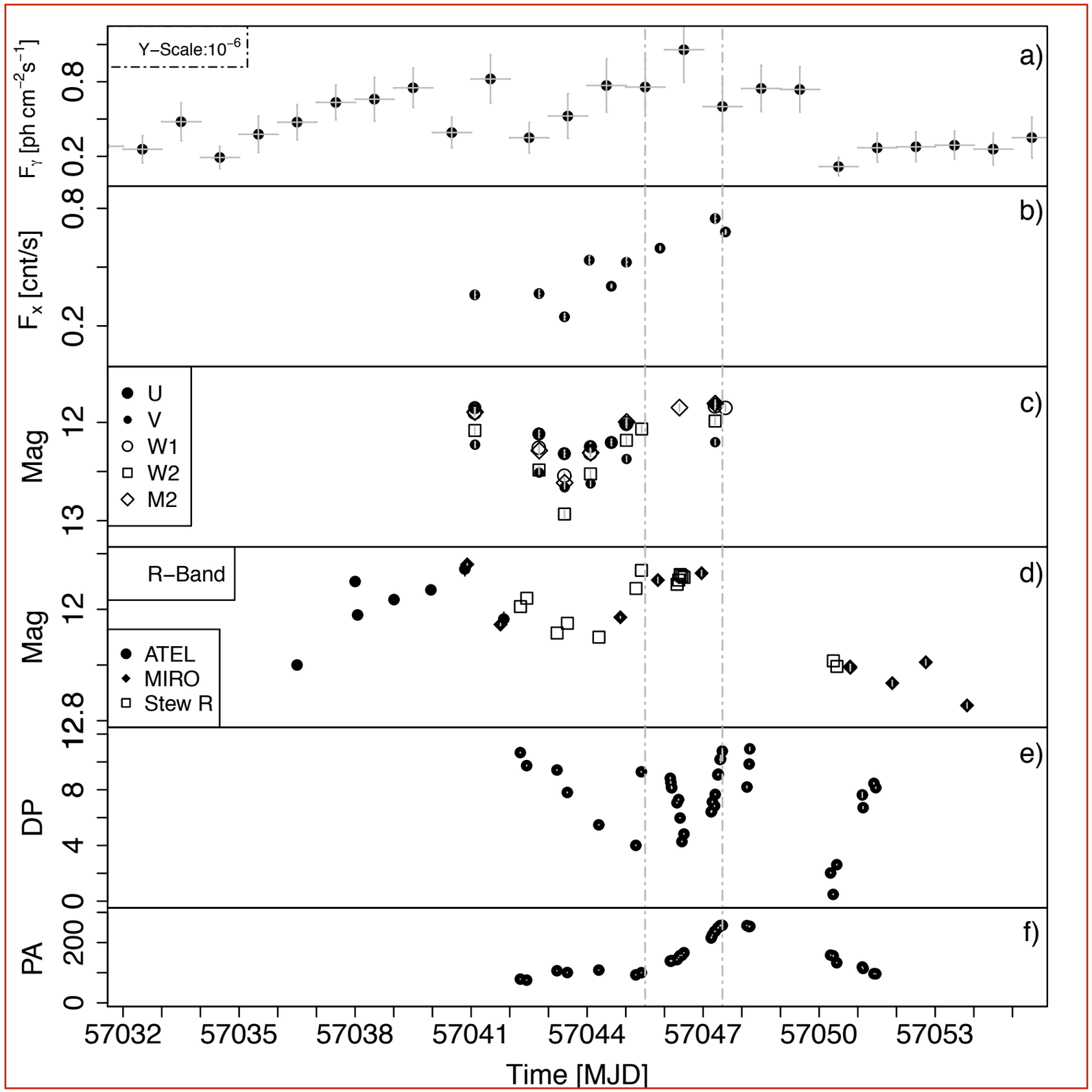

Multi-wavelength Lightcurves S5 0716+714 (z~0.31), 2015 January 23 - February 03

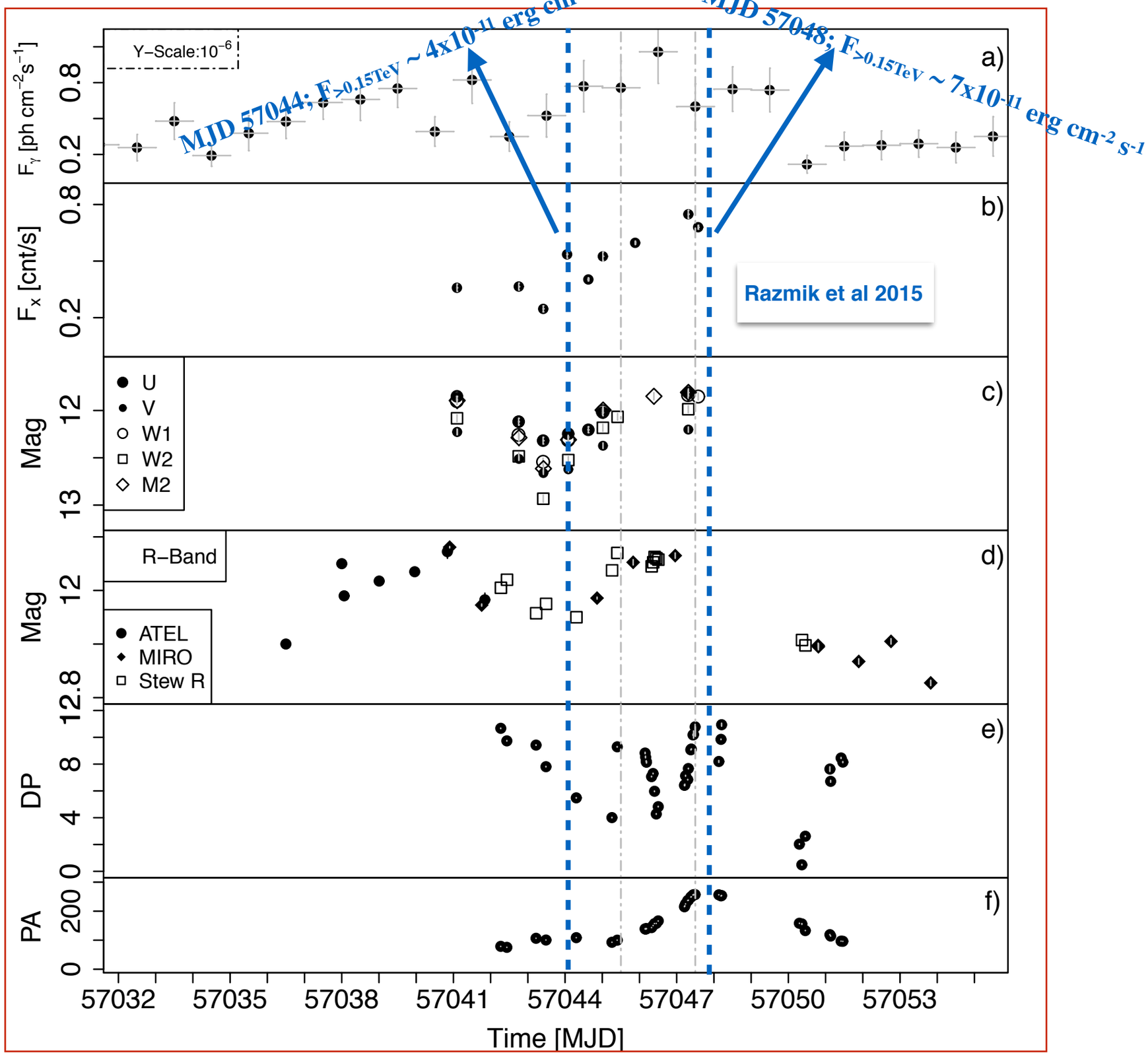

Color Dependence and Flux-Flux Correlations in Optical band

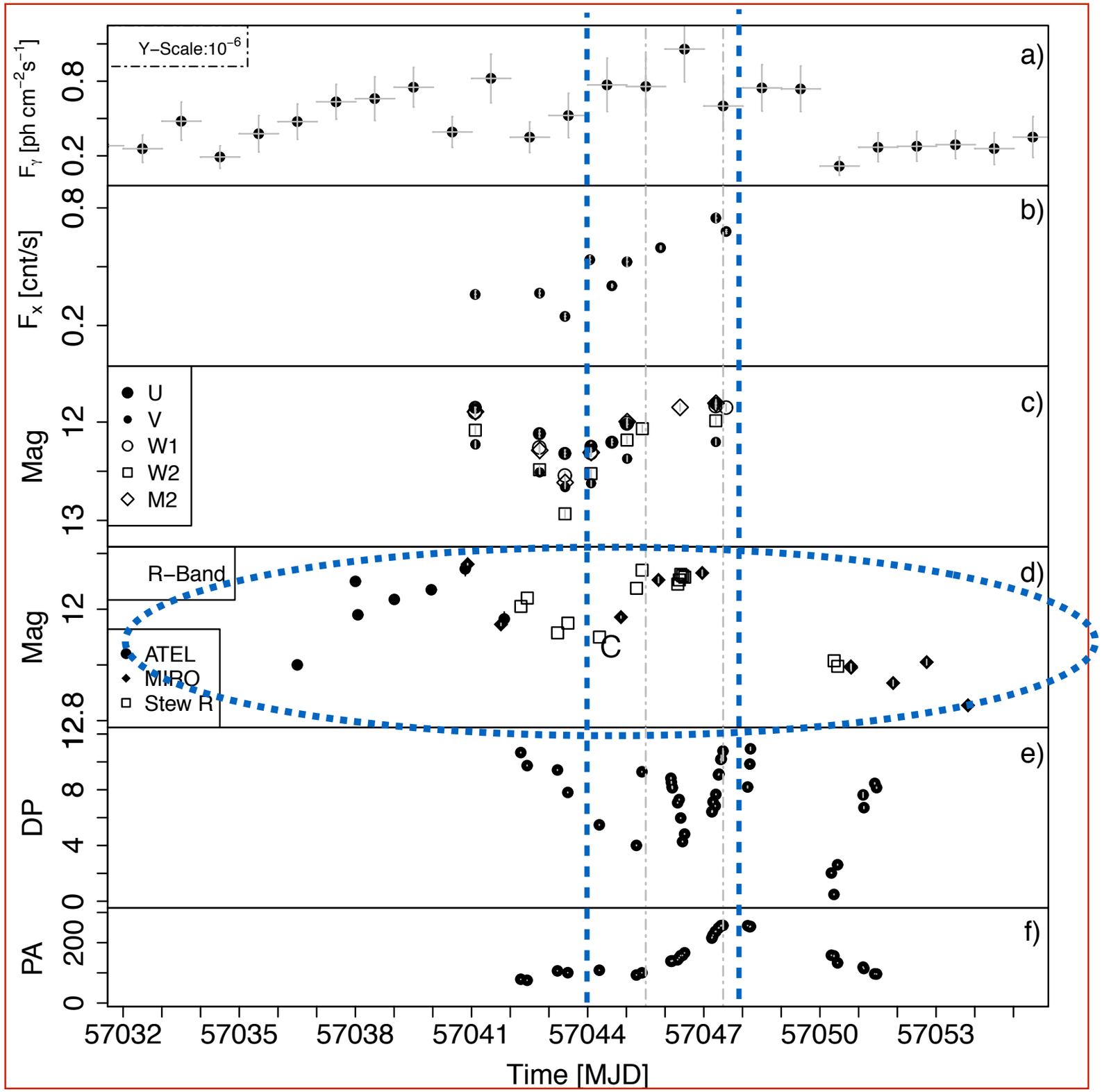

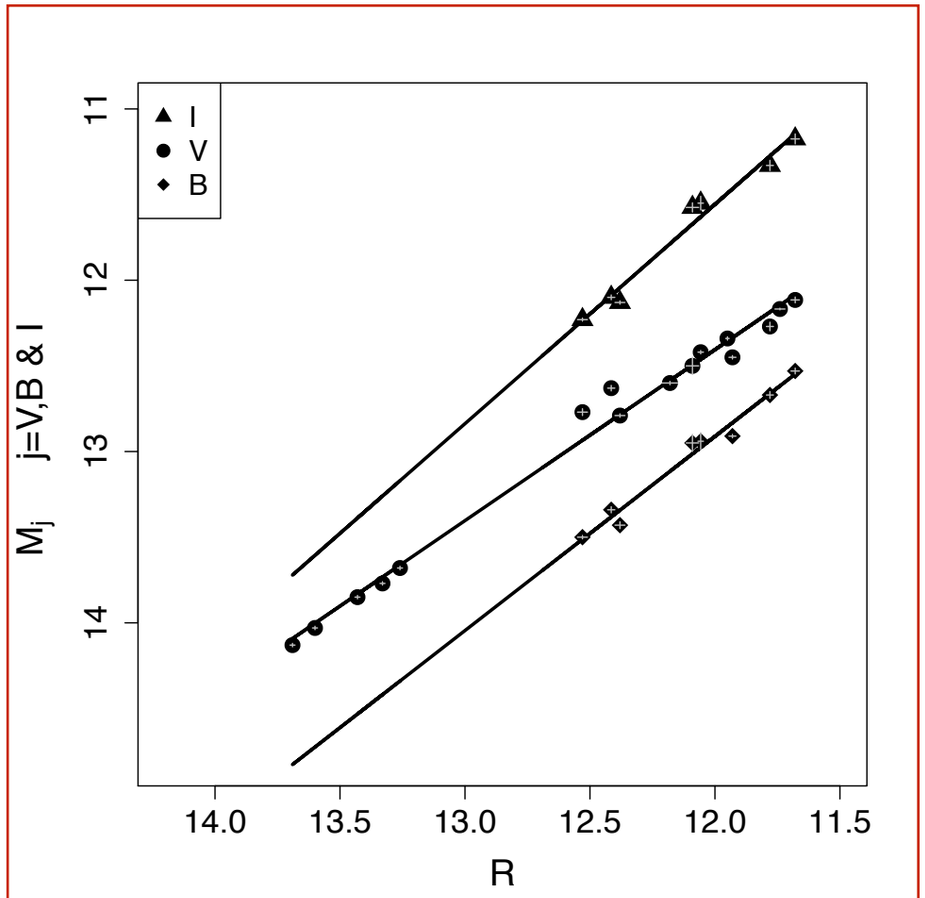

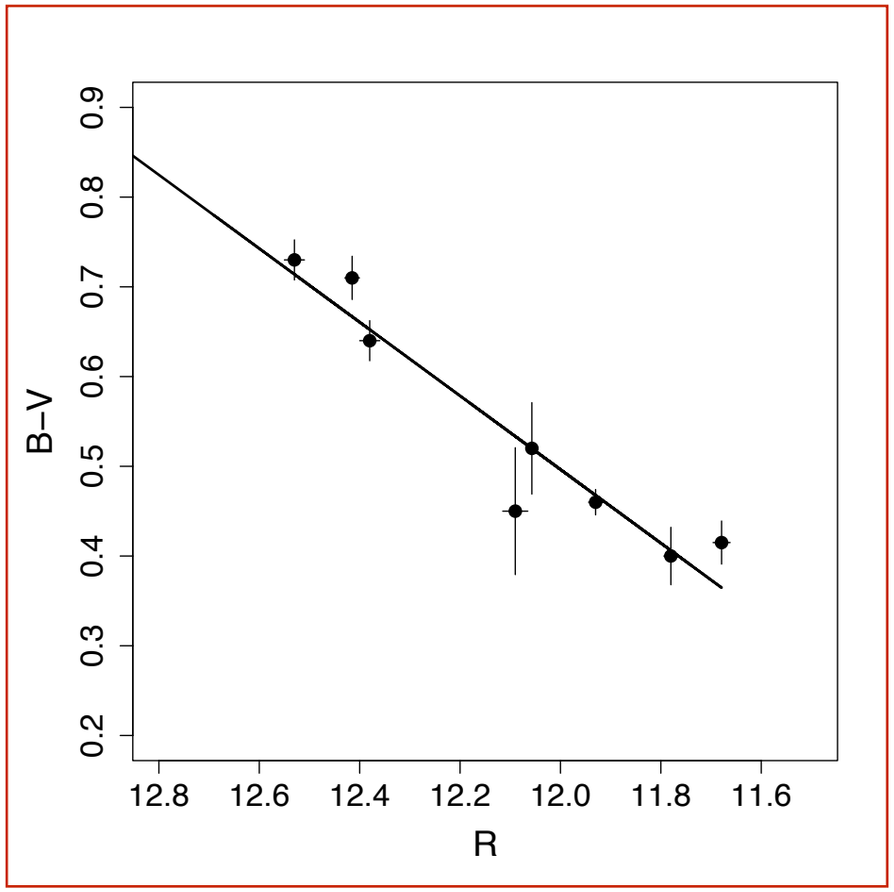

Color Dependence and Flux-Flux Correlations in Optical band

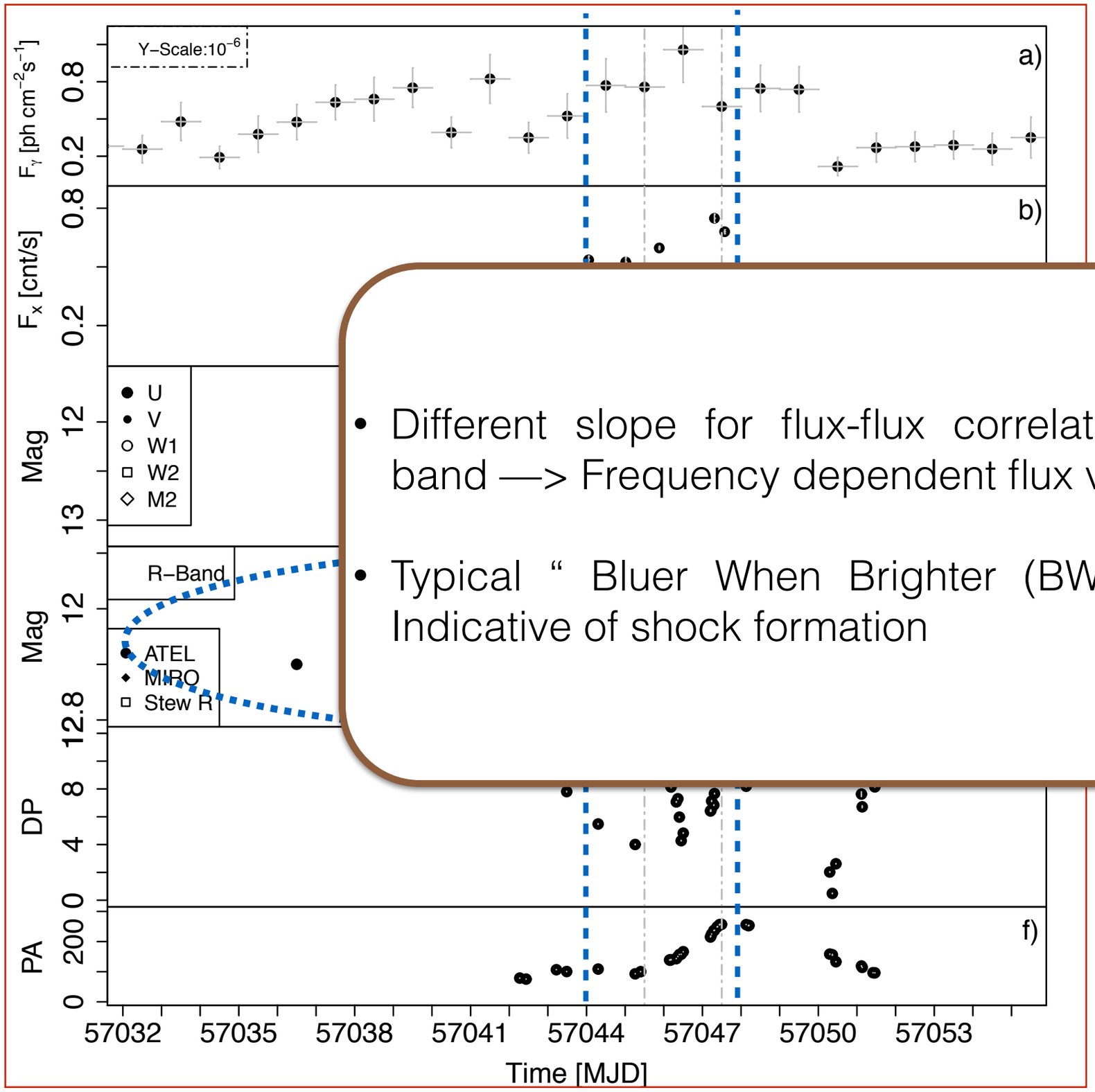

- Different slope for flux-flux correlation for different band —> Frequency dependent flux variations
- Typical “ Bluer When Brighter (BWB) ” trend —> Indicative of shock formation

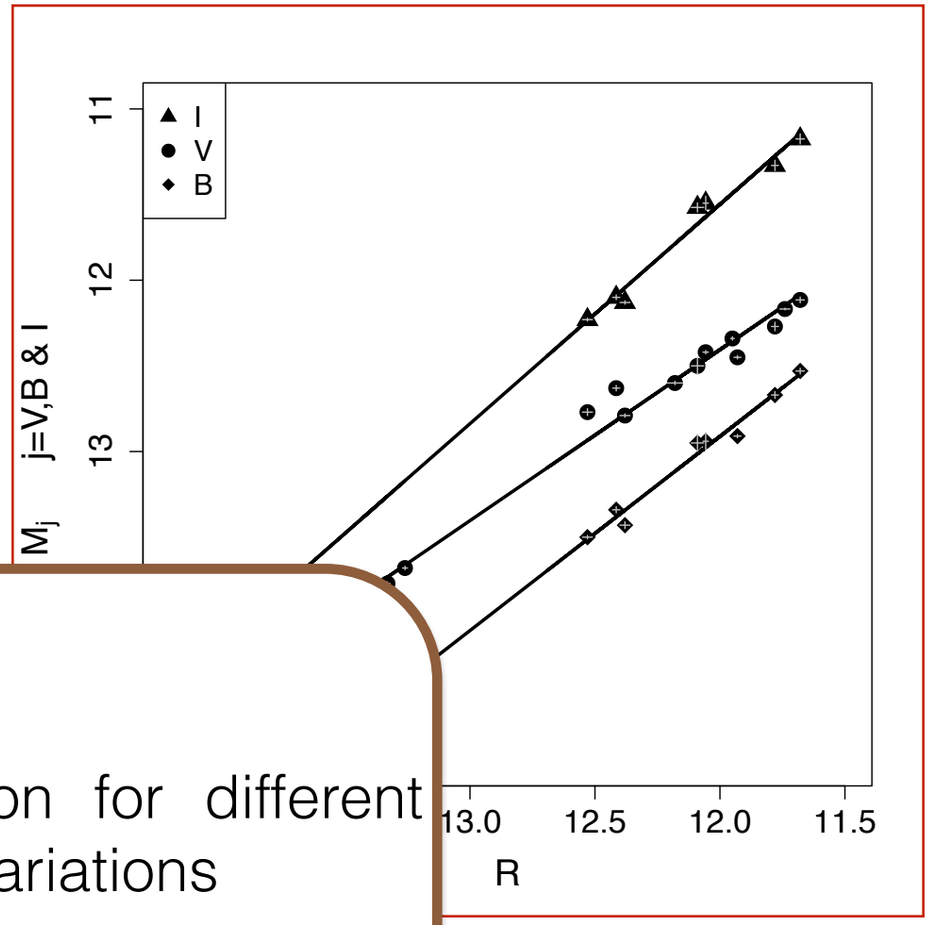

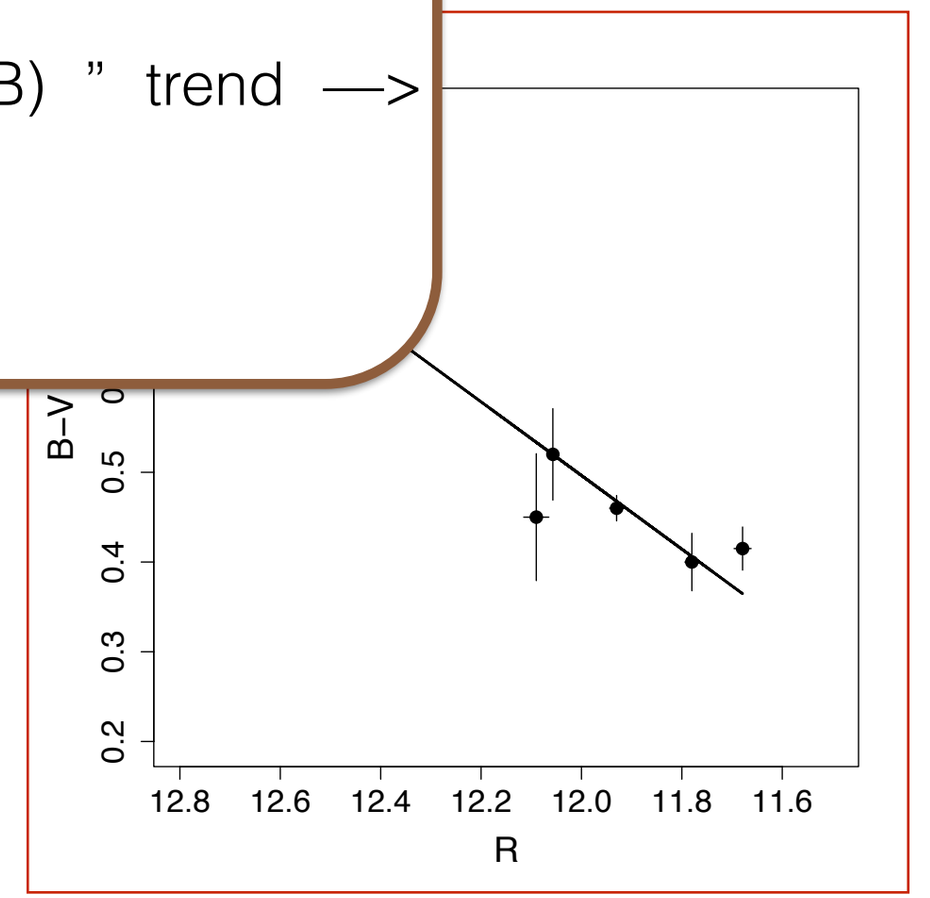

Degree of Polarization and Position angle during outburst

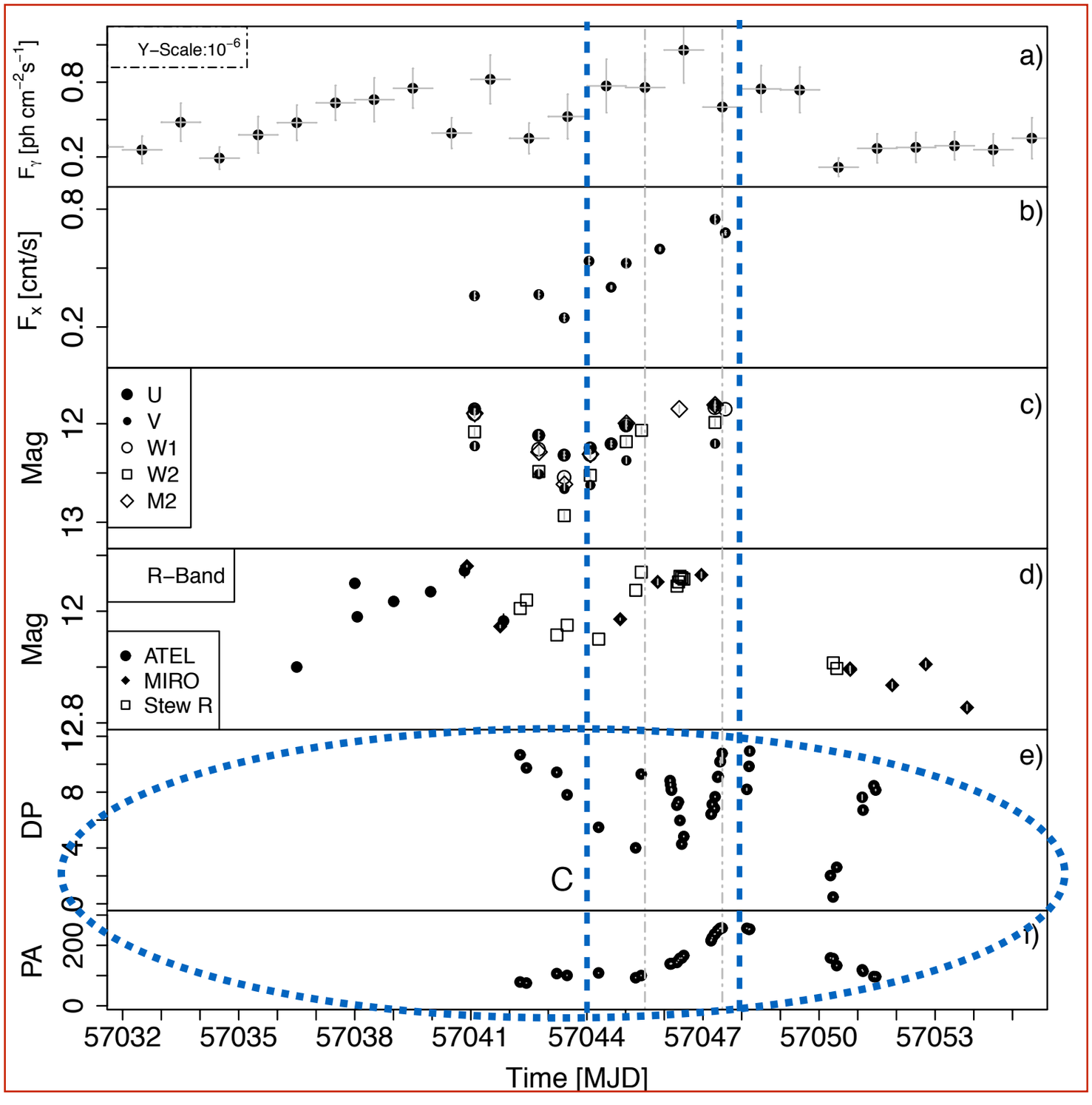

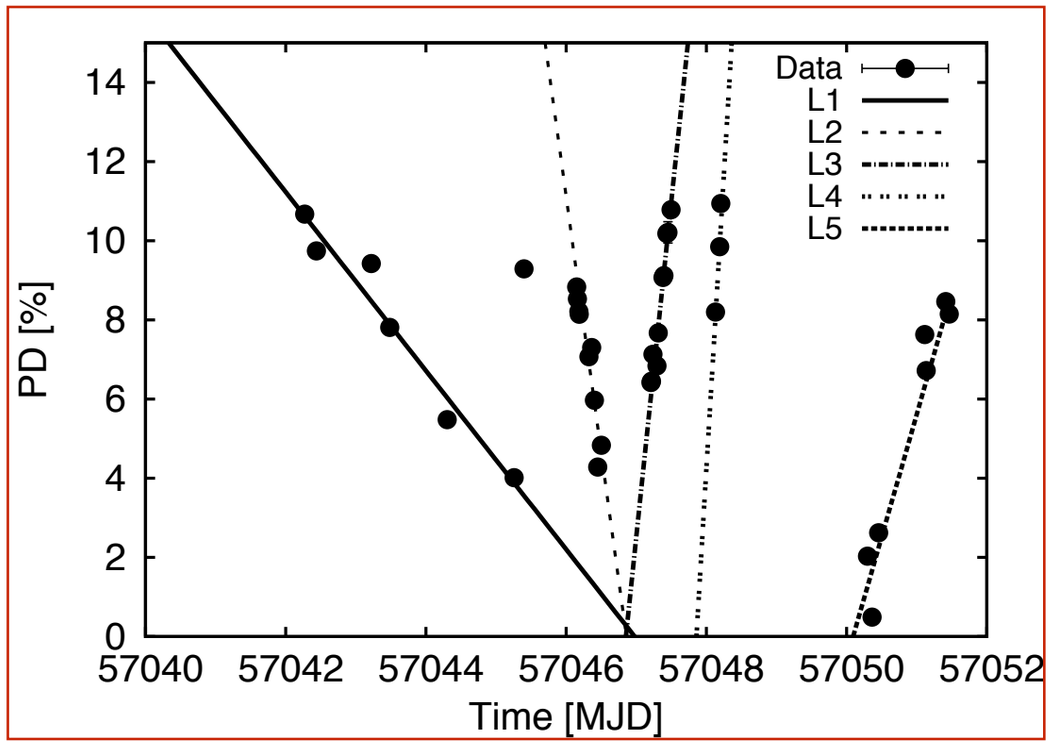

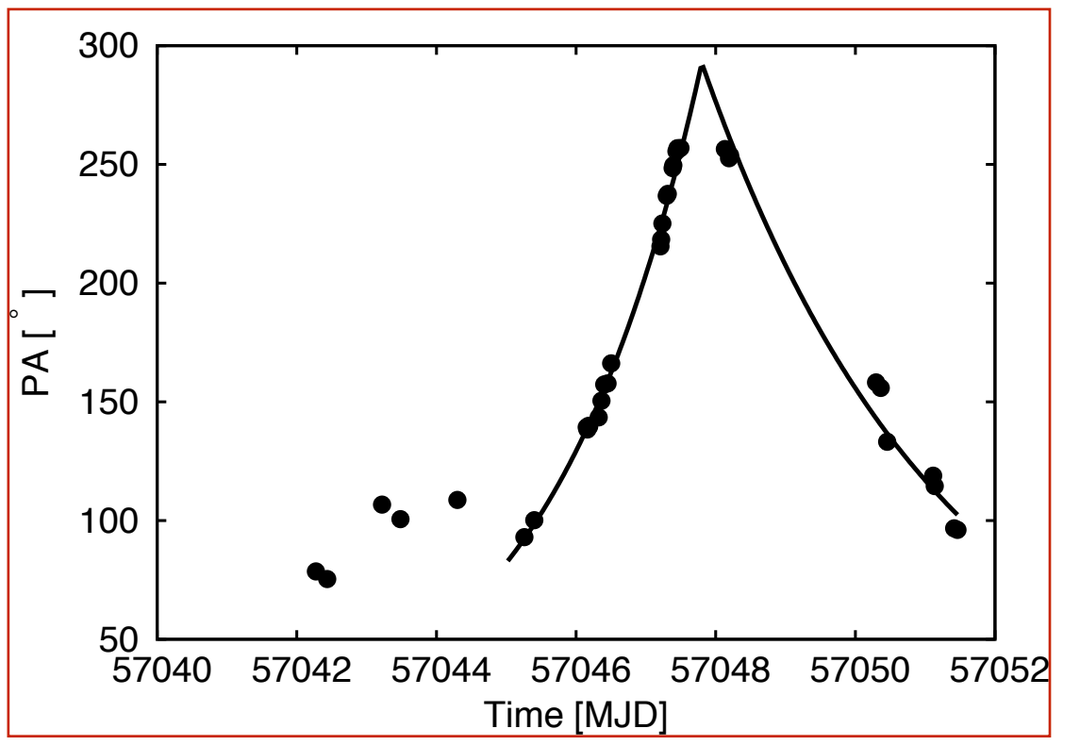

Degree of Polarization and Position angle during outburst

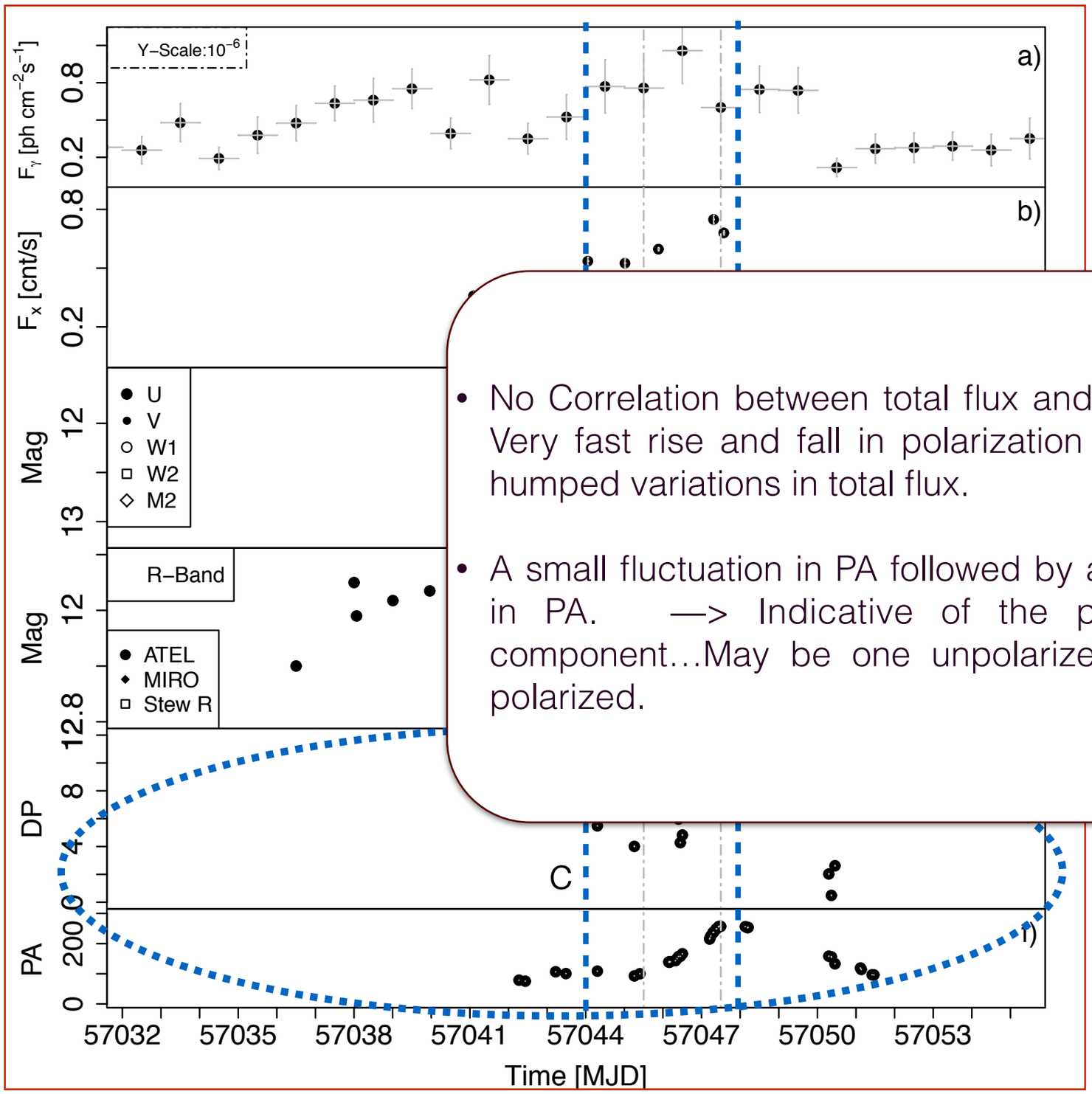

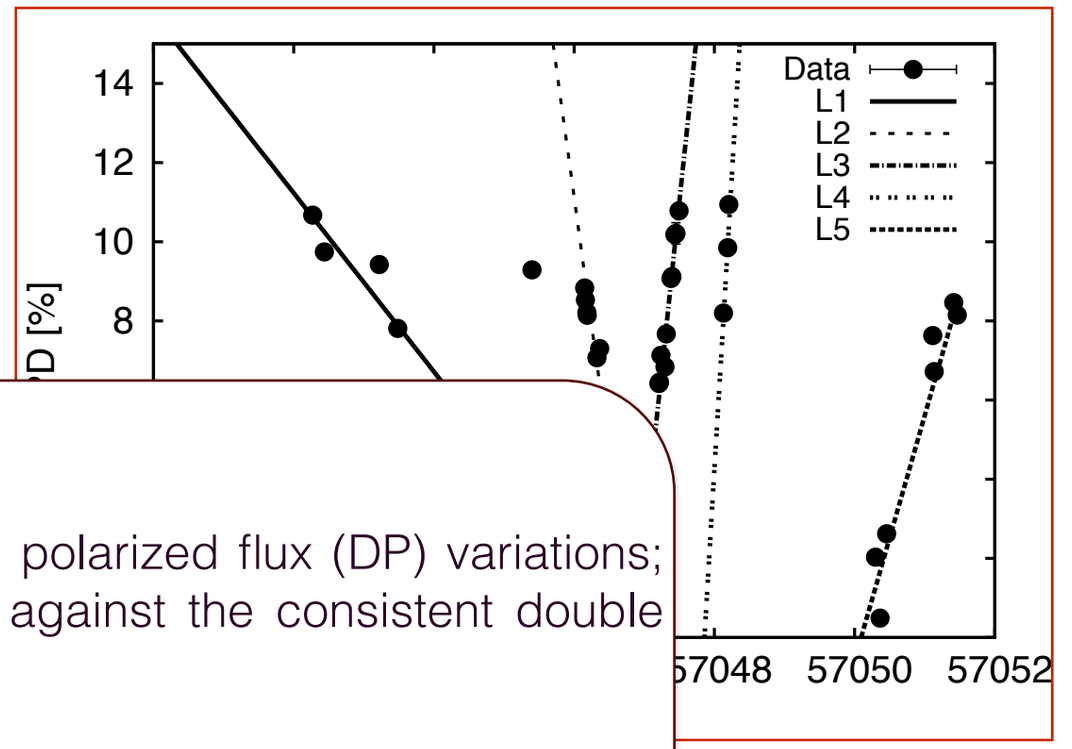

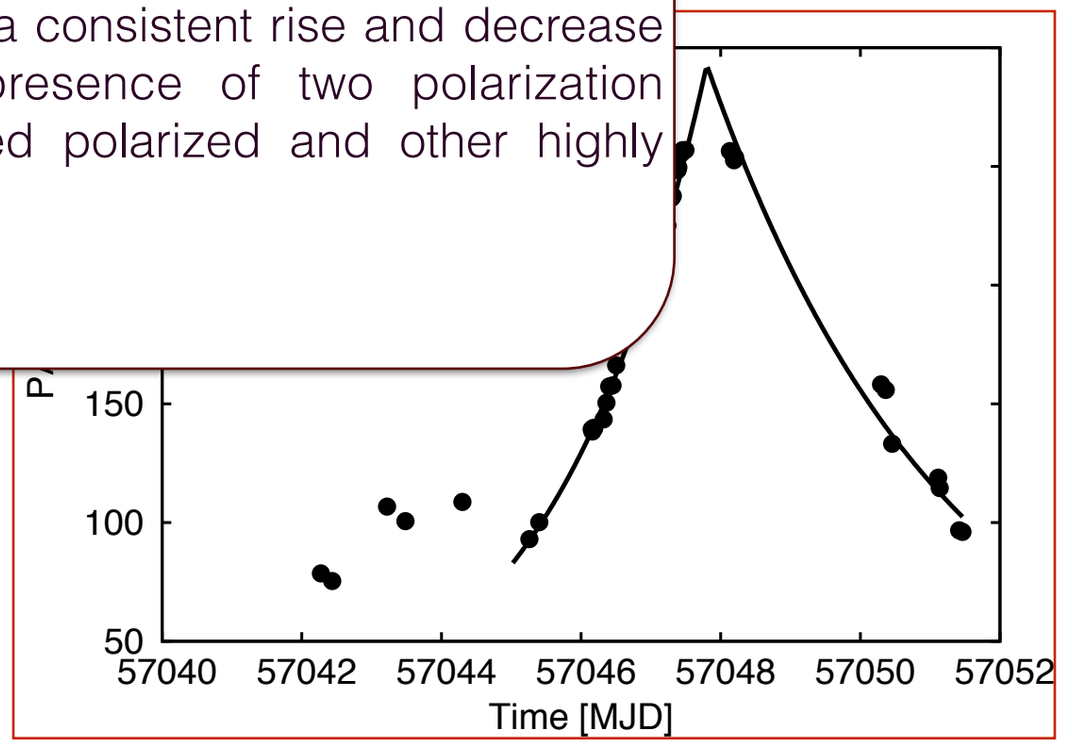

- No Correlation between total flux and polarized flux (DP) variations; Very fast rise and fall in polarization against the consistent double humped variations in total flux.
- A small fluctuation in PA followed by a consistent rise and decrease in PA. —> Indicative of the presence of two polarization component…May be one unpolarized polarized and other highly polarized.

Degree of Polarization and Position angle during outburst

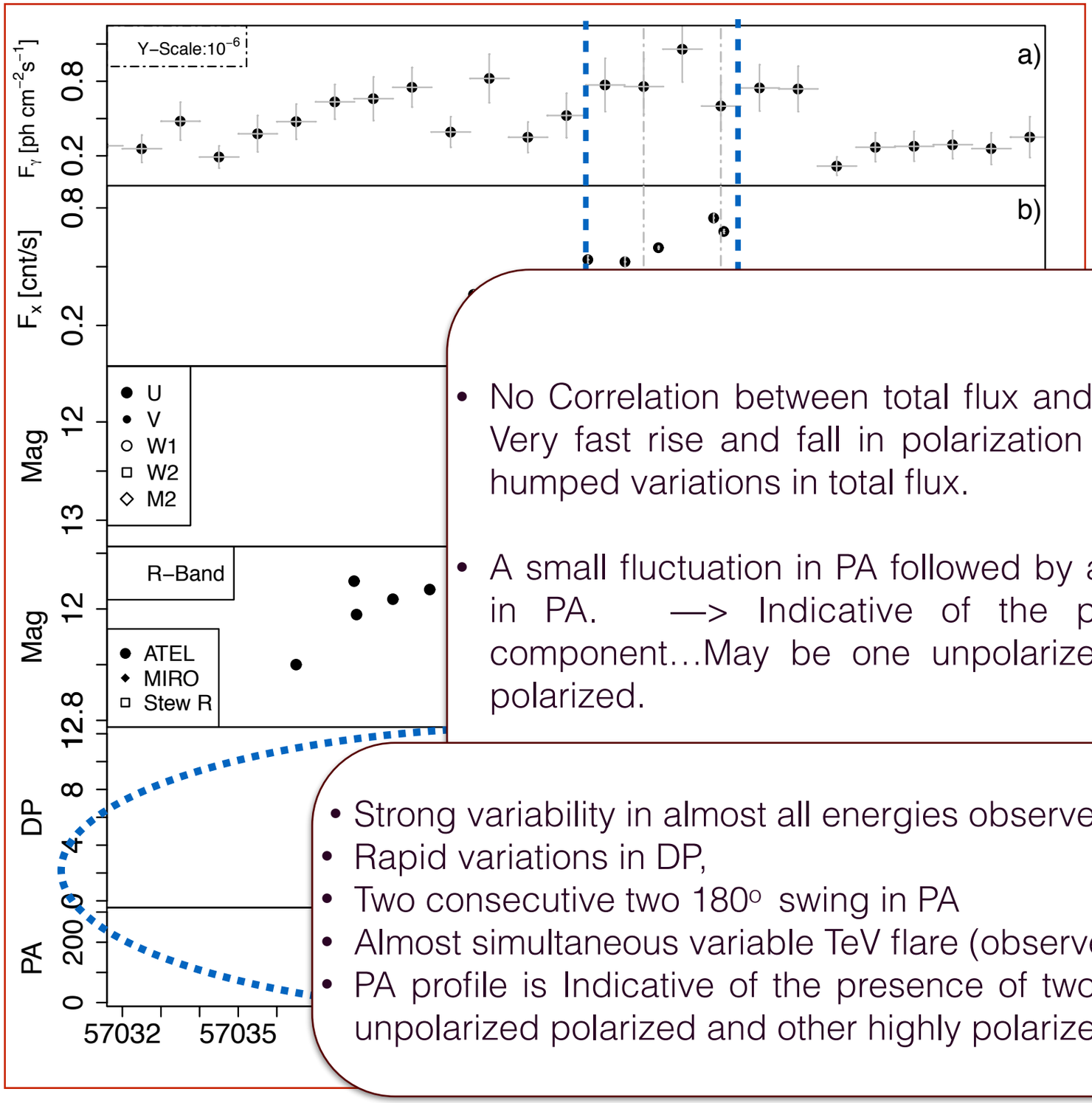

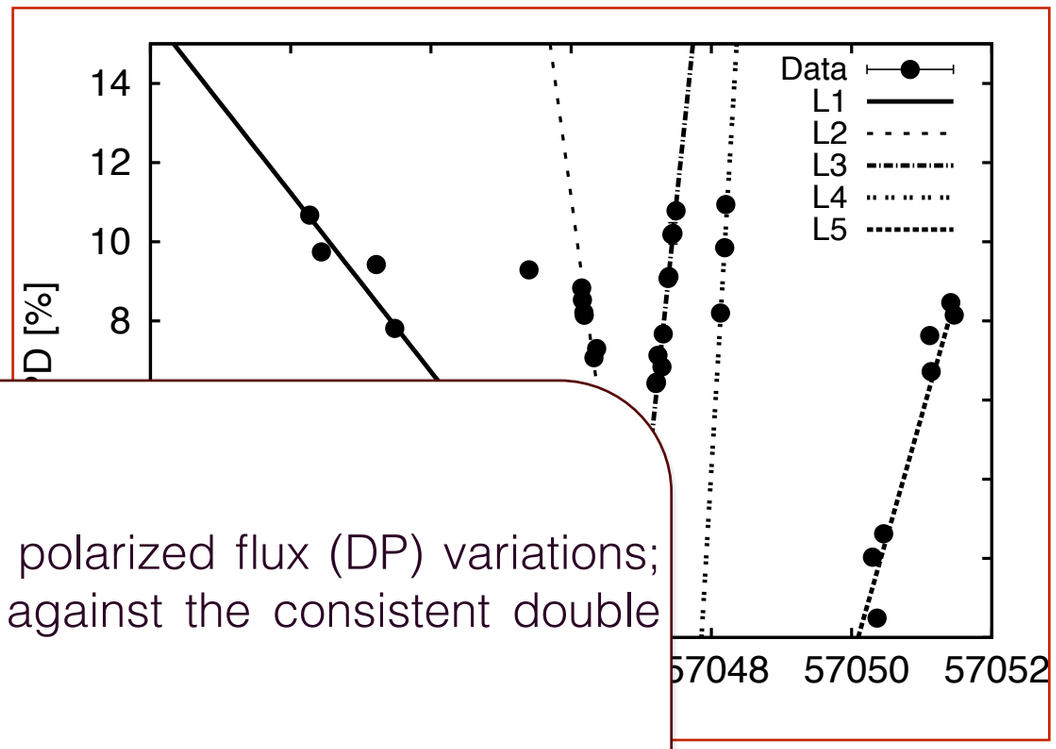

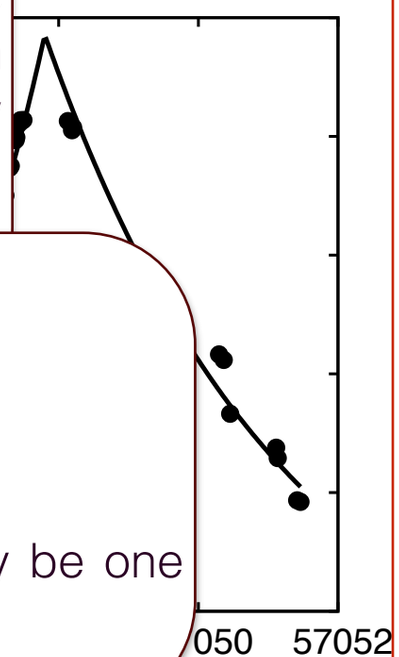

- No Correlation between total flux and polarized flux (DP) variations; Very fast rise and fall in polarization against the consistent double humped variations in total flux.
- A small fluctuation in PA followed by a consistent rise and decrease in PA. —> Indicative of the presence of two polarization component…May be one unpolarized polarized and other highly polarized.

- Strong variability in almost all energies observed.
- Rapid variations in DP,
- Two consecutive two 180^o swing in PA
- Almost simultaneous variable TeV flare (observed by MAGIC)
- PA profile is Indicative of the presence of two polarization component…May be one unpolarized polarized and other highly polarized.

Degree of Polarization and Position angle during outburst

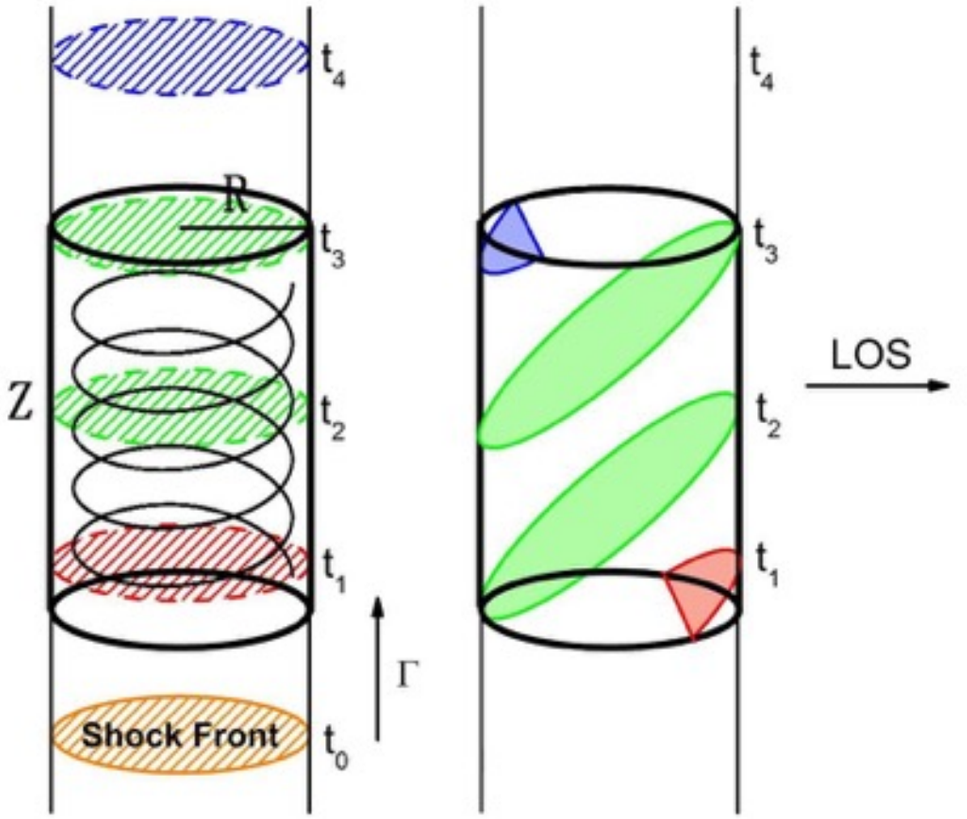

The simultaneous data during MJD 57045.5-57047.5 are used. The light curves at almost all the energies seems to be constant.

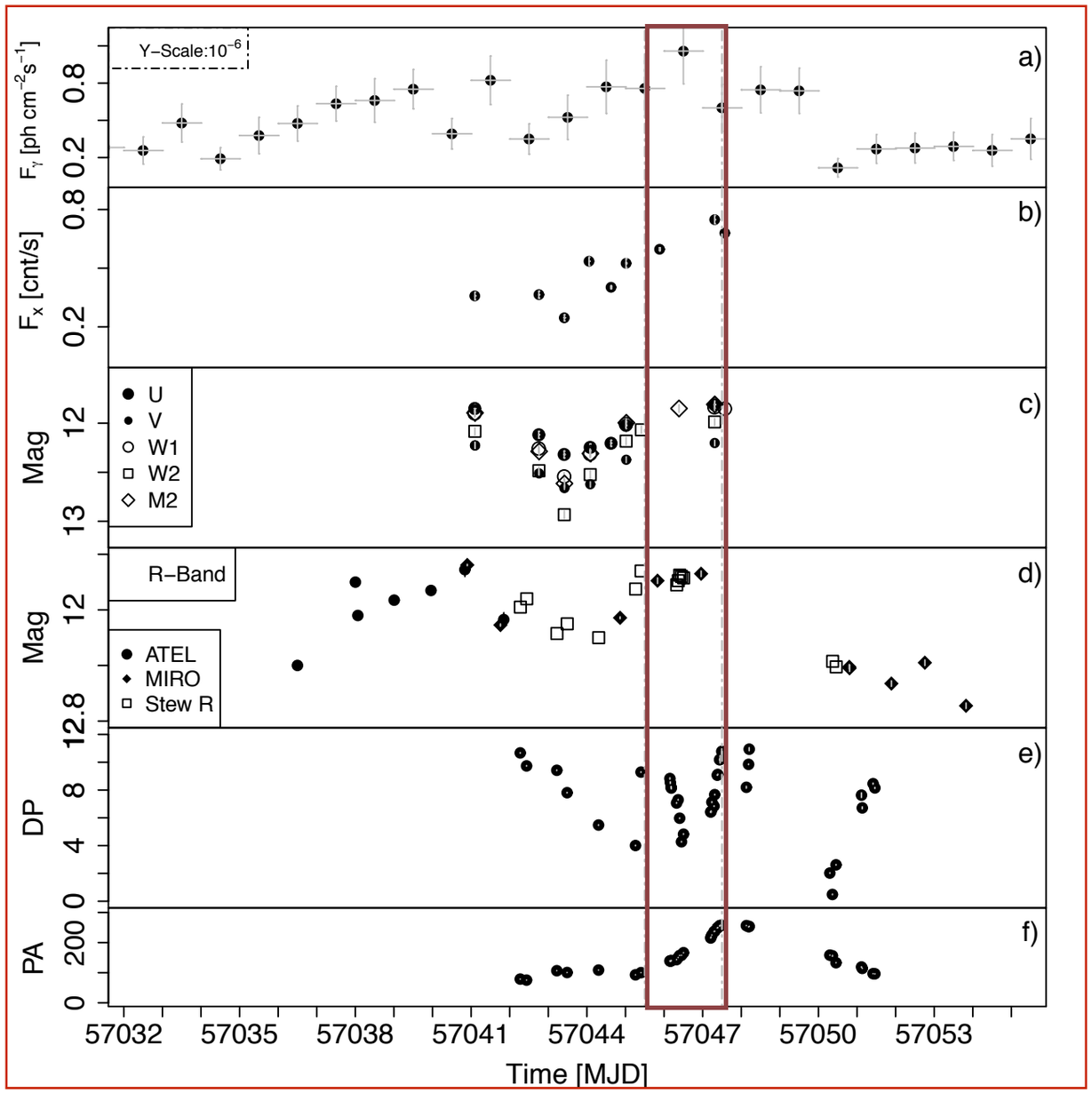

Re-produced SED and polarization

The Light-curves are not shown here. Because they are almost constant for the duration of our interest
Second rotation could not be modelled because of poor data

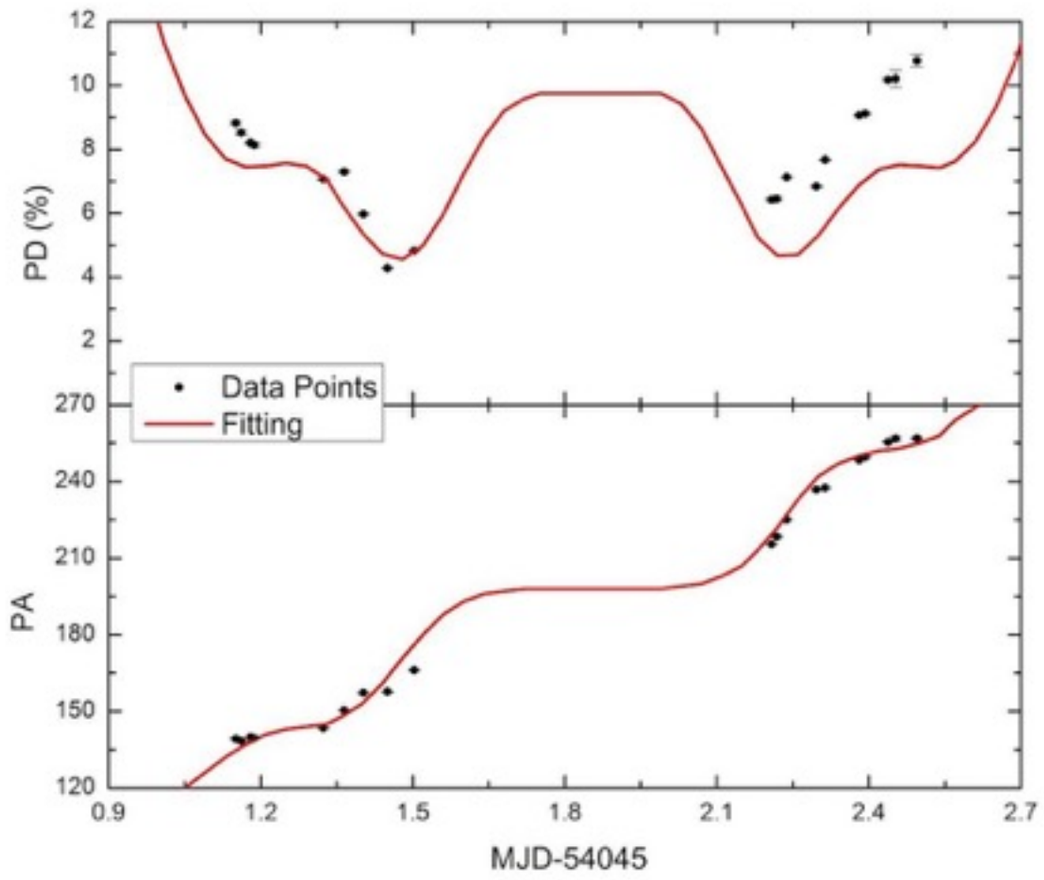

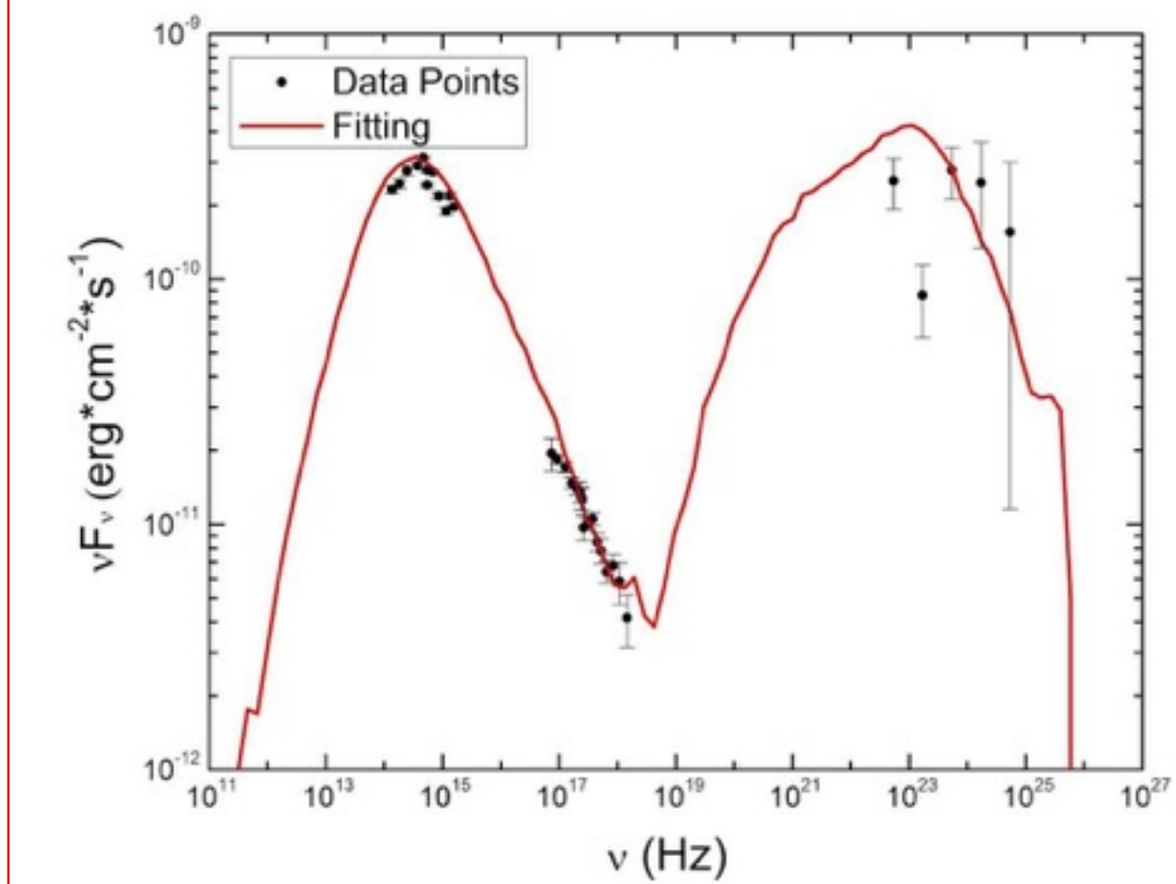

Re-produced SED and polarization

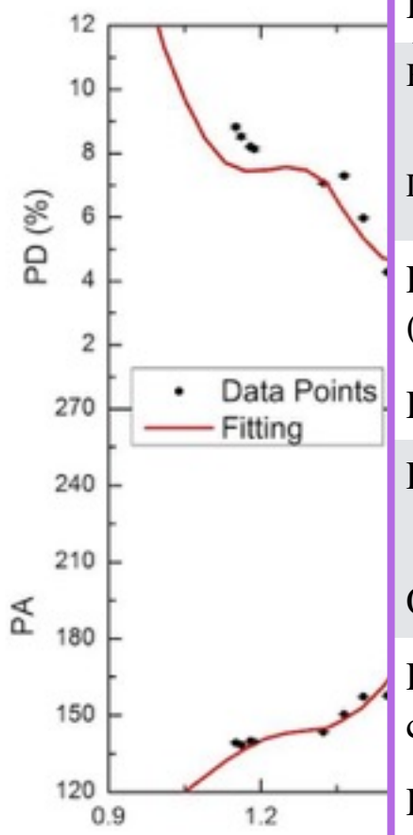

Parameters	Values
Helical pitch angle (deg)	47
Helical pitch angle during flare	75.5
Bulk Lorentz factor	20
Length of the emission region Z (cm)	6.06×10^{16}
Radius of the emission region R (cm)	2.25×10^{16}
Length of the disturbance L (cm)	6.06×10^{15}
Radius of the disturbance A (cm)	2.25×10^{16}
Orientation of LOS (deg)	90
Electron acceleration time-scale (Z/c)	5.50×10^{-3}
Electron escape time-scale (Z/c)	6.00×10^{-4}
Electron density (cm^{-3})	21.7
Helical magnetic field strength (G)	0.5

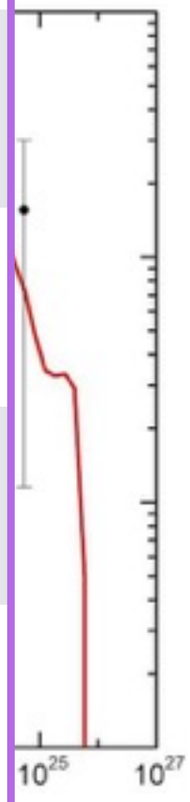

Three channels:
130-180 nm, 180-300 nm, and 320-530 nm.
The field of view ~ 28 arcmin
angular resolution: 1.8" for the ultraviolet channels
and 2.5" for the visible channel
Low resolution slit-less NUV/FUV spectra (R ~ 100)

UVIT (IIA+IUCAA+TIFR)

Wolter-I type
Focal length: 2m
Field of view: 41.3 x 41.3 arcmin
Pixel Scale: 4.13 arcsec/pixel
Energy Range: 0.3 – 8.0 keV
Effective Area: 200 cm2 @1.5 keV
20 cm2 @6.5 keV

SXT (TIFR)

LAXPC (TIFR)

Field of View of 1°x1°
energy band of 3-80 keV
Detection Efficiency : 100% below 15 keV
and about 50 % up to 80 keV
Combined Effective Area: 6000 cm² at 5 keV

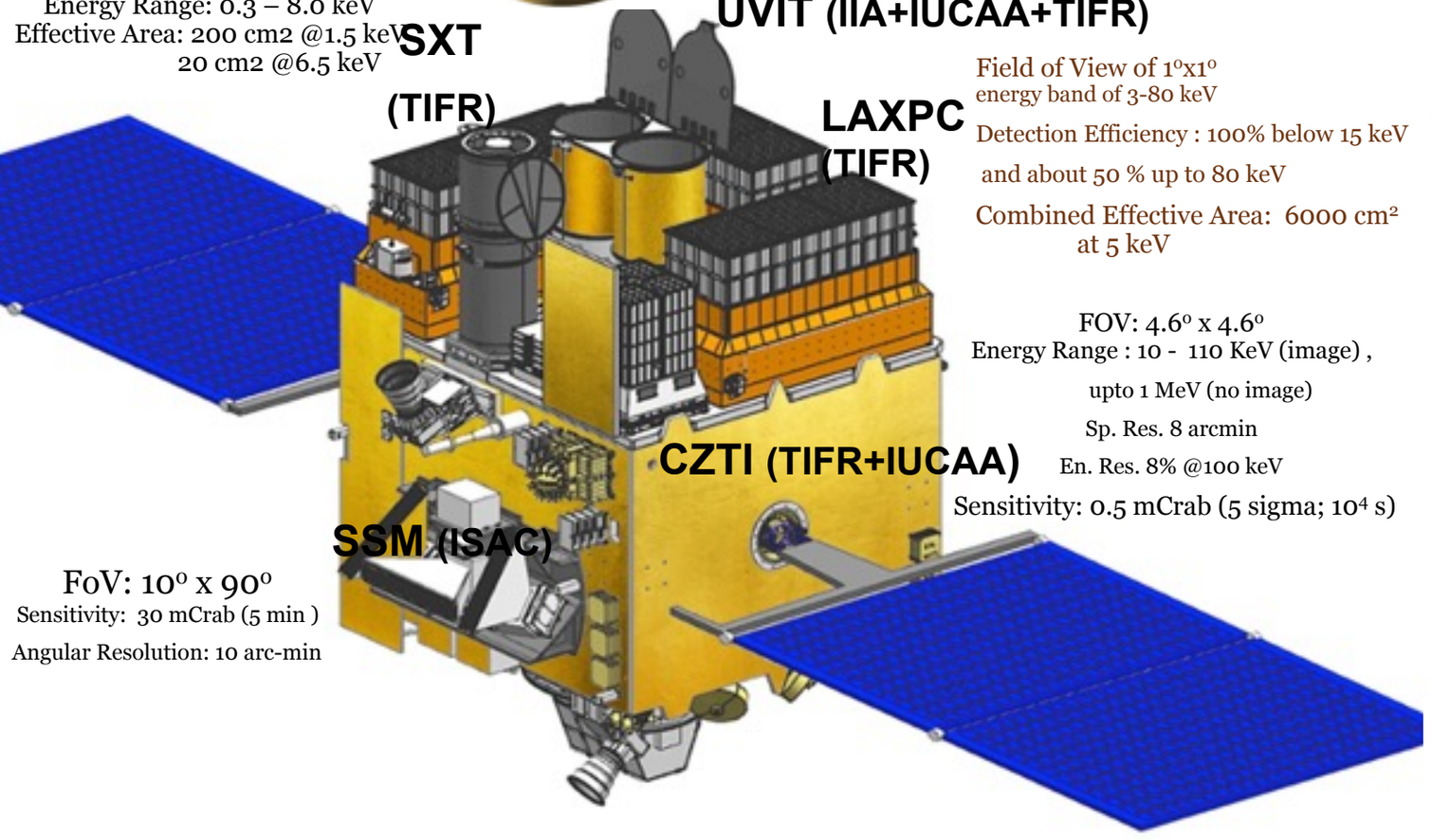

FOV: 4.6° x 4.6°
Energy Range : 10 - 110 KeV (image) ,
upto 1 MeV (no image)
Sp. Res. 8 arcmin
En. Res. 8% @100 keV
Sensitivity: 0.5 mCrab (5 sigma; 10^4 s)

CZTI (TIFR+IUCAA)

SSM (ISAC)

FoV: 10° x 90°
Sensitivity: 30 mCrab (5 min)
Angular Resolution: 10 arc-min

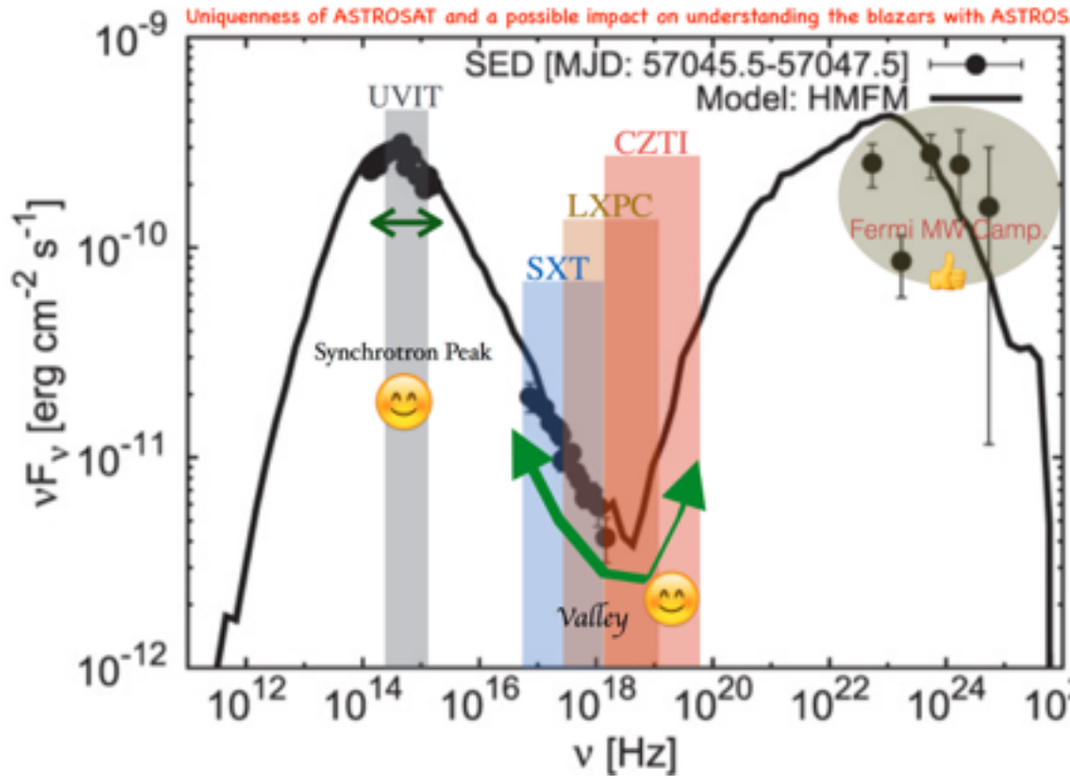

Launched On : 28 September 2015

ASTROSAT/LAXPC REVEALS THE HIGH ENERGY VARIABILITY OF GRS 1915+105 IN THE χ CLASS

J S Yadav[1], Ranjeev Misra[2], Jai Verdhan Chauhan[1], P C Agrawal[3], H M Antia[1], Mayukh Pahari[2], Dhiraj Dedhia[1], Tilak Katoch[1], P. Madhwani[1], R K Manchanda[4], B Paul[5], Parag Shah[1], C H Ishwara-Chandra[6]
[1] Tata Institute of Fundamental Research, Homi Bhabha Road, Mumbai, India; jsyadav@tifr.res.in
[2] Inter-University Centre for Astronomy and Astrophysics, Pune 411007, India
[3] UM-DAE Center of Excellence for Basic Sciences, University of Mumbai, Kalina, Mumbai-400098, India
[4] University of Mumbai, Kalina, Mumbai-400098, India
[5] Dept. of Astronomy & Astrophysics, Raman Research Institute, Bengaluru-560080 India and
[6] National Center for Radio Astrophysics, Pune 411007, India

Draft version August 25, 2016

https://arxiv.org/pdf/1608.07023.pdf

ASTROSAT CZT IMAGER OBSERVATIONS OF GRB 151006A: TIMING, SPECTROSCOPY, AND POLARISATION STUDY

A. R. Rao[1], Vikas Chand[1], M.K. Hingar[1], S. Iyyani[1], Rakesh Khanna[1], A.P.K. Kutty[1], J.P. Malkar[1], D. Paul[1], V. B. Bhalerao[2], D. Bhattacharya[2], G. C. Dewangan[2], Pramod Pawar[2,3], A. M. Vibhute[2], T. Chattopadhyay[4], N.P.S. Mithun[4], S.V. Vadawale[4], N. Vagshette[4], R. Basak[5], P. Pradeep[6], Essy Samuel[6], S. Sreekumar[6], P. Vinod[6], K.H. Navalgund[7], R. Pandiyan[7], K. S. Sarma[7], S. Seetha[7] K. Subbarao[7]

arxiv.org/abs/1608.07388

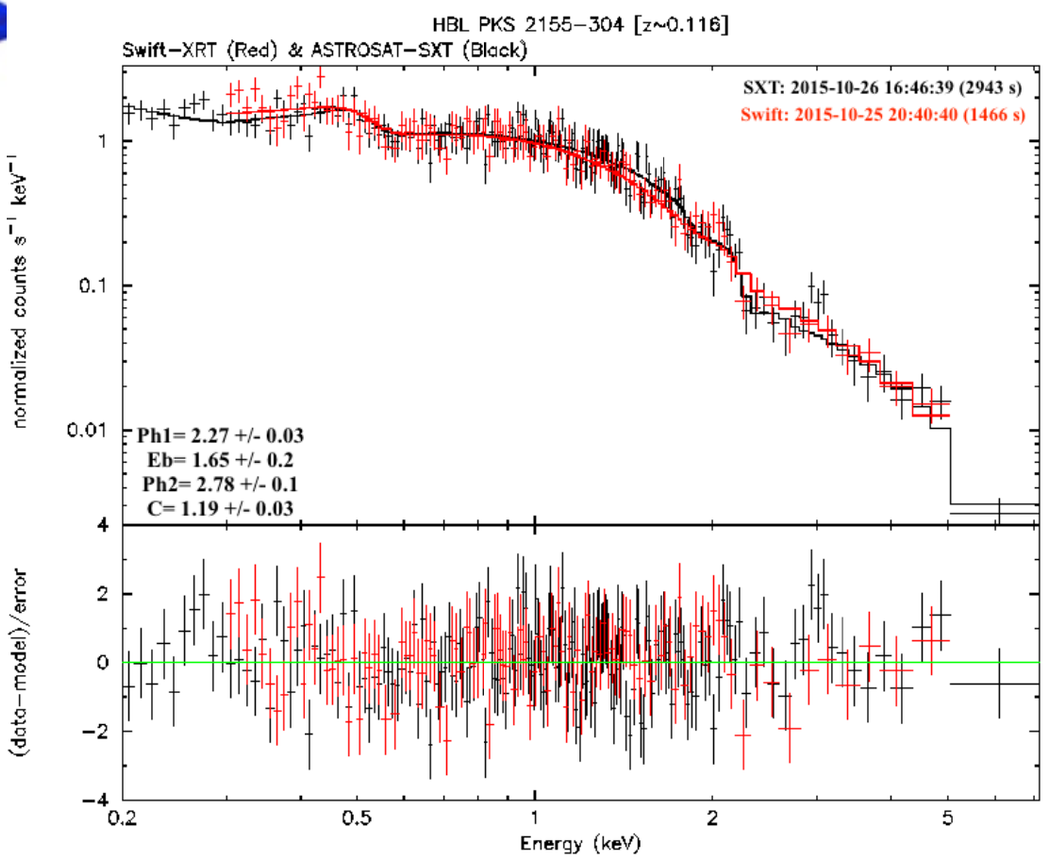

Wolter-I type
Focal length: 2m
Field of view: 41.3 x 41.3 arcmin
Pixel Scale: 4.13 arcsec/pixel
Energy Range: 0.3 – 8.0 keV
Effective Area: 200 cm2 @1.5 keV
20 cm2 @6.5 keV

SXT

(TIFR)

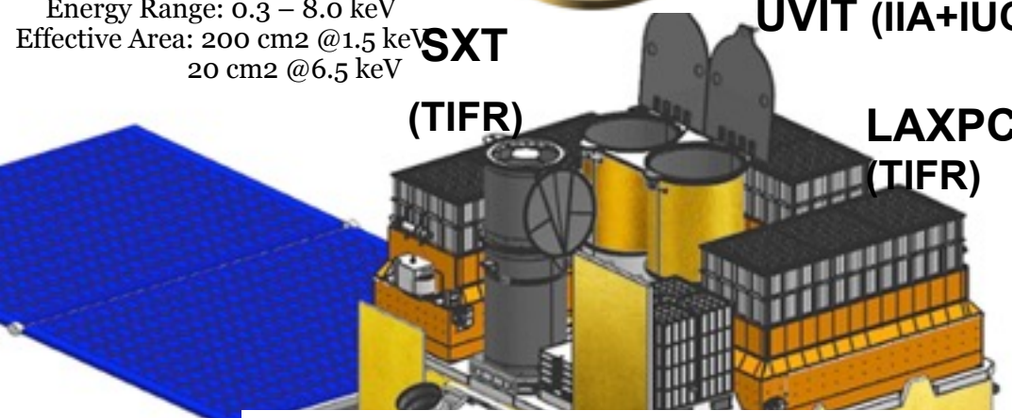

Three channels:
130-180 nm, 180-300 nm, and 320-530 nm.
The field of view ~ 28 arcmin
angular resolution: 1.8" for the ultraviolet channels
and 2.5" for the visible channel
Low resolution slit-less NUV/FUV spectra (R ~ 100)

UVIT (IIA+IUCAA+TIFR)

LAXPC
(TIFR)

Field of View of 1°x1°
energy band of 3-80 keV
Detection Efficiency : 100% below 15 keV
and about 50 % up to 80 keV
Combined Effective Area: 6000 cm² at 5 keV

FOV: 4.6° x 4.6°
Energy Range : 10 - 110 KeV (image) ,

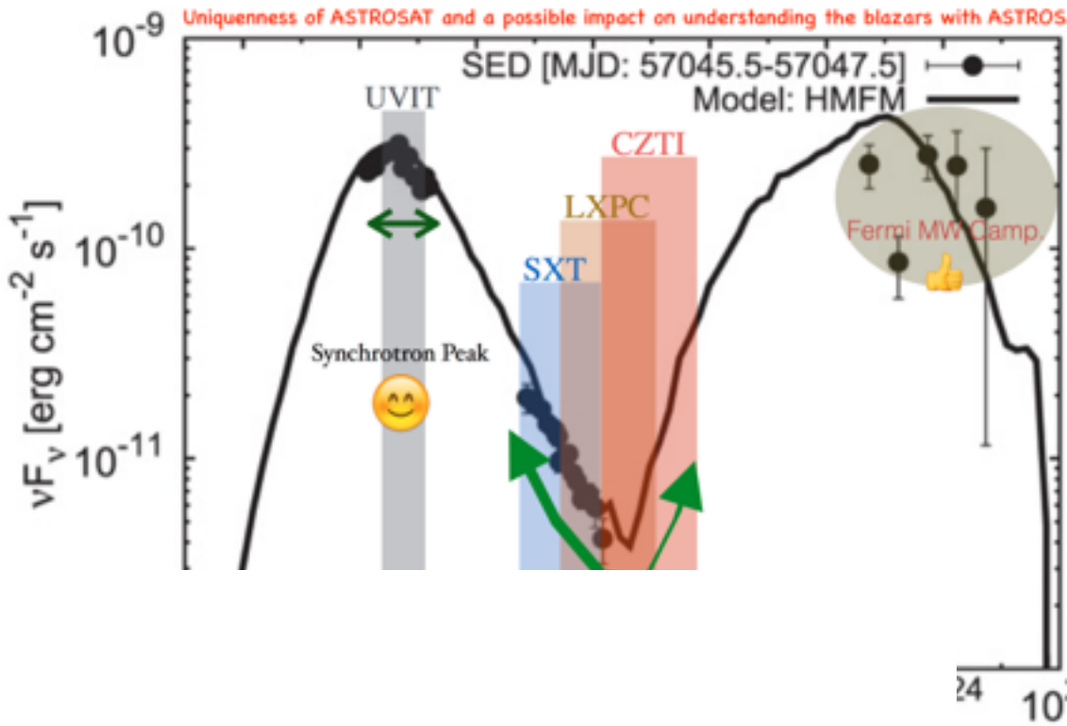

FoV: 10° x 9

Sensitivity: 30 mCrab

Angular Resolution: 1(

THANK YOU FOR YOUR KIND ATTENTION

ASTROSAT/LAX

J S Yadav[1], Ran.
Dedhia[1], Tilak
[1] Tat
[3] UM-I
5

ASTROSAT CZT IMAGER OBSERVATIONS OF GRB 151006A: TIMING, SPECTROSCOPY, AND POLARISATION STUDY

A. R. Rao[1], Vikas Chand[1], M.K. Hingar[1], S. Iyyani[1], Rakesh Khanna[1], A.P.K. Kutty[1], J.P. Malkar[1], D. Paul[1], V. B. Bhalerao[2], D. Bhattacharya[2], G. C. Dewangan[2], Pramod Pawar[2,3], A. M. Vibhute[2], T. Chattopadhyay[4], N.P.S. Mithun[4], S.V. Vadawale[4], N. Vagshette[4], R. Basak[5], P. Pradeep[6], Essy Samuel[6], S. Sreekumar[6], P. Vinod[6], K.H. Navalgund[7], R. Pandiyan[7], K. S. Sarma[7], S. Seetha[7] K. Subbarao[7]

arxiv.org/abs/1608.07388

We are open for collaborations :
sunil.chandra355@gmail.com